



# รายงานวิจัยฉบับสมบูรณ์

โครงการการพัฒนาวิธีการตรวจจับการเจาะทะลุสำหรับการ ผ่าตัดกระดูกที่ต้องการความเที่ยงตรงสูง

โดย ผู้ช่วยศาสตราจารย์ ดร. ภิญโญ พวงมะลิ

กรกฎาคม 2563

# สัญญาเลขที่ MRG5980212

# รายงานวิจัยฉบับสมบูรณ์

โครงการการพัฒนาวิธีการตรวจจับการเจาะทะลุสำหรับการ ผ่าตัดกระดูกที่ต้องการความเที่ยงตรงสูง

ผศ.ดร.ภิญโญ พวงมะลิ มหาวิทยาลัยเชียงใหม่

สนับสนุนโดยสำนักงานกองทุนสนับสนุนการวิจัยและต้นสังกัด

(ความเห็นในรายงานนี้เป็นของผู้วิจัย สกว. และต้นสังกัดไม่จำเป็นต้องเห็นด้วยเสมอไป)

## บทคัดย่อ

รหัสโครงการ: MRG5980212

ชื่อโครงการ: การพัฒนาวิธีการตรวจจับการเจาะทะลุสำหรับการผ่าตัดกระดูกที่ต้องการ

ความเที่ยงตรงสูง

**ชื่อหักวิจัย :** ภิญโญ พวงมะลิ มหาวิทยาลัยเชียงใหม่

E-mail Address: pinyo@dome.eng.cmu.ac.th

ระยะเวลาโครงการ : 2 พฤษภาคม 2559 – 1 พฤษภาคม 2562

ในการผ่าตัดกระดูกนั้น การเจาะกระดูกโดยไม่ทำให้เกิดความเสียหายอย่างหนักต่อเนื้อ เยื้อต่างๆ เป็นกระบวนการที่มีความสำคัญอย่างมาก โดยเฉพาะอย่างยิ่งสำหรับการผ่าตัดกะโหลก ศีรษะ กระดูกสันหลัง และกระดูกที่มีความพิเศษเฉพาะ กระบวนการเจาะกระดูกยิ่งต้องมีความ แม่นยำและเที่ยงตรงสูง ทั้งนี้เนื่องจากการเจาะทะลุเกินระยะที่ต้องการสามารถทำความเสียหาย ต่อเส้นประสาท เส้นเลือด และอวัยวะโดยรอบ ดังนั้นเพื่อเป็นการเพิ่มความปลอดภัยในการเจาะ เทคนิคการตรวจจับการเจาะทะลุแบบใหม่ซึ่งไม่มีการติดตั้งเซนเซอร์สำหรับการตรวจวัดแรงและ แรงบิดดังที่นิยมทำในงานวิจัยอื่นจึงถูกนำเสนอ เทคนิคดังกล่าวนี้อาศัยเพียงการตรวจวัด กระแสไฟฟ้าที่ใหลไปยังมอเตอร์ของสว่านไฟฟ้าเท่านั้น จากการวัดปริมาณกระแสไฟฟ้าขณะที่ทำ การเจาะแบบทีละขั้นและการประยุกต์ใช้ขั้นตอนวิธีที่มีการตั้งค่าเทรชโฮลด์เปรียบเทียบแบบ ฮีสเตอรีซีสทำให้การเจาะทะลุสามารถถูกบ่งชี้ได้ตามเวลาจริงอย่างมีประสิทธิภาพ การทดสอบใน ห้องปฏิบัติการด้วยเครื่องเจาะต้นแบบที่ใช้เทคนิคดังกล่าวนี้แสดงให้เห็นว่าการเจาะทะลุสามารถ ถูกตรวจจับได้อย่างคงตัว ซึ่งสิ่งนี้ช่วยป้องกันการเจาะเกินได้ ส่งผลทำให้การเจาะมีความเชื่อถือ ได้ในแง่ที่สามารถจำกัดความเสียหายต่อเนื้อเยื่อต่างๆ ให้เกิดขึ้นน้อยที่สุด อย่างไรก็ตาม ข้อจำกัด ของวิธีการนี้คือจำเป็นต้องมีการปรับตั้งค่าพารามิเตอร์ในการตรวจจับใหม่สำหรับการเจาะกระดูก ชนิดต่างๆ รวมทั้งกรณีของการเจาะที่ใช้ขนาดและรูปร่างของดอกสว่านต่างกัน การศึกษาประเด็น ้ปัญหานี้และประเด็นปัญหาอื่นๆ เช่น ผลกระทบจากความเร็วการหมุนของหัวสว่าน ความกระด้าง ของแท่นสว่าน และความกระด้างของตัววัตถุที่ถูกเจาะ ยังเป็นสิ่งจำเป็นสำหรับการวิจัยในอนาคต เพื่อปรับปรุงการตั้งค่าเทรชโฮลด์ให้ดียิ่งขึ้น

**คำหลัก**: การเจาะกระดูก การตรวจจับการเจาะทะลุ การตรวจจับการทะลุออก การตรวจจับการ ผ่านทะลุ การควบคุมการผ่านทะลุ

#### **Abstract**

Project Code: MRG5980212

Project Title: Development of a Breakthrough Detection Scheme for Precise

**Bone Surgery** 

Investigator: Pinyo Puangmali, Chiang Mai University

**E-mail Address :** pinyo@dome.eng.cmu.ac.th

Project Period: 2<sup>nd</sup> May 2016 – 1<sup>st</sup> May 2019

In bone surgery, drilling of bone without causing severe damage to tissue is a critical procedure. Particularly for skull, spine, and special kinds of orthopedic surgeries, the process of bone drilling requires high accuracy and precision since excessive drill protrusion can cause damage to nerves, blood vessels, and nearby organs. To enhance safety of drilling, a new breakthrough detection technique that does not require the installation of a sensor for force or torque measurement as usually done in other research is proposed. This technique relies only on the measurement of current flowing through the motor of an electric drill to monitor drilling progress. By measuring the amount of current while executing stepwise drilling and applying a hysteresis thresholding algorithm, the breakthrough event can be effectively identified in real-time. Experimental tests of a drill prototype utilizing this scheme showed that breakthrough could be consistently detected. This prevents over drilling, enabling reliable drilling operation which can minimize tissue damage. However, the main limitation of this scheme is that tuning of detection parameters for specific bone types and drilling conditions such as using different drill bit sizes and shapes is required. Further investigations on these issues including the effects of spindle speed, stiffness of the drill stand, and stiffness of the drilled object itself are also required for improving threshold setting.

**Keywords:** Bone drilling; Breakthrough detection; Breakout detection; Penetration detection; Penetration control.

#### **Executive Summary**

#### 1. Introduction

Surgery is commonly used to treat disease and abnormalities of bones such as bone tumors, malignant bones, impaired bone joints, and disorders of tissues adjacent to the bones. The most common case is as treatment for repairing broken bones. To cure the fracture of bones, the surgeon usually performs drilling and scaffolding. However, because bones are quite rigid and difficult to cut and drill, performing such surgical procedures requires delicate skills and special tools.

In general cases of surgery, tools for drilling bones are handheld devices that are designed to operate with compressed air or electricity. Such traditional tools are portable, convenient to use, and efficient, but one of their drawbacks is that they do not have built-in safety mechanisms to ensure safe usage. The safety of drilling relies only on the perception of the surgeon. Thus, how well the surgeon can apply the tools greatly depends on his/her experience and expertise. In many critical drilling operations such as skull and spine drilling, even a small mistake can cause serious damage to blood vessels, nerves, and nearby organs. In extreme cases, this may result in paralysis or death. The surgeon must therefore be extremely careful when applying a drilling tool close to sensitive organs.

At present, advances in electronic and computer technology enable the development of high performance drilling equipment for bone surgery. To enhance safety, many drilling devices equipped with sensing instruments have been developed. Several bone-breakthrough detection schemes have also been proposed. However, the accuracy and precision of breakthrough detection still requires further improvement, especially for critical surgical operations.

#### 2. Objectives

- To find an effective means for bone breakthrough detection in bone drilling operation.
- To develop a breakthrough detection system that can perform bone breakthrough detection with high reliability.

 To develop a bone drilling tool that can be used to carry out precise surgical procedures.

#### 3. Methodology

Breakthrough detection can be performed based on the measurement of physical quantities that change during the operation of drilling. One of the useful quantities is the electrical current flowing to the motor driving the drill spindle. Based on a former study of electrical drill characteristics, it was found that an increment of drilling torque load while drilling causes the motor to consume more current. However, when the breakthrough is occurring, the torque load declines, causing the current to reduce simultaneously. In principle, this phenomenon allows breakthrough to be detected based on the monitoring only of the motor current. A simple indicator for identifying the breakthrough involves a threshold value which can be determined slightly higher than the amount of current at no load. When the current flowing to the motor diminishes to such a value (usually during the occurrence of the breakthrough), the breakthrough is detected.

Breakthrough detection based on current measurement is considered an effective approach since, in typical set-ups, the current responds to torque load change very quickly. The measurement of current is also simple since it can be carried out without need of modifying the structure of the drill to install a sensor. Instead, it can be realized by connecting the drill with a current sensing circuit. However, a major concern on measuring current is that the current measurement signal usually noisy due to commutation noise and electrical interference in the power lines of motor system. Using current measurement signal to perform breakthrough detection therefore requires special techniques to treat the signal before it can be used as an indicator for detecting a breakthrough.

This research focused on finding an effective way to apply current measurement to perform breakthrough detection. To carry out research, 4 main consecutive tasks were planned

 Study of drilling mechanics: A part of research work involved in the analysis of dynamics of drilling. A mathematical model of an electric drill was derived and analyzed for this purpose. This work led to the understanding on the effects of drilling parameters and torque-current relationship.

- 2) Developing a new breakthrough detection technique: Based on the study of drilling mechanics, torque-current relationship and the limitations on performing current measurement were analyzed. Appropriate hardware and software were then designed for facilitating drilling and performing breakthrough detection.
- 3) Developing a drill prototype: A prototype that can perform accurate drilling was designed, built, and tested. Mechanical hardware was mainly designed for facilitating drilling operation while electrical hardware and associated software embedded with breakthrough detection algorithm were mainly designed for breakthrough detection. All these were integrated to form a system of the drill prototype.
- 4) Testing the prototype: The drill prototype and its associated components was used to test the breakthrough detection capability. The performance of the drilling system was quantitatively assessed, especially on the aspect of the repeatability of detecting the breakthrough. The results of the tests were then analyzed for further improvement.

#### 4. Research Results

In this research, it was found that effective breakthrough detection in bone drilling processes can be achieved based on the combination of three key techniques: 1) measurement of current flowing though the motor of the electric drill using a sense resistor with a specially designed optoelectronic circuit, 2) stepwise drilling action controlled by a microcontroller, and 3) hysteresis thresholding for breakthrough detection with noise immunity. The measurement of current can be performed effectively by applying a sense resistor with specially designed signal conditioning circuit, which is composed of an isolation amplifier, a unity-gain differential amplifier with input filter components, and an instrumentation amplifier. With the stepwise drilling action, there is a peak in the current measurement signal at each step of drilling. By monitoring the peak, the breakthrough can be identified since, when the breakthrough begins to occur, the peaks at successive drilling steps decline. If the peak declines below threshold values according to the hysteresis thresholding principle, the breakthrough is detected. The drilling operation can then be immediately terminated before excessive drill protrusion occurs.

#### 5. Outputs

New knowledge and technique for detecting bone breakthrough which can be applied for designing a high-performance smart surgical device for bone surgery. A newly developed drill prototype which was used to conduct experiments in the laboratory demonstrated the applicability of the proposed breakthrough detection technique.

#### 6. Outcome

Puangmali, P., Jetdumronglerd, S., Wongratanaphisan, T. and Cole, M.O., "Sensorless stepwise breakthrough detection technique for safe surgical drilling of bone." Mechatronics 65 (2020): 102306. (Q1, Impact Factor 2.992)

# Acknowledgements

I am very grateful for the financial support from the Thailand Science Research and Innovation (formerly Thailand Research Fund), Thailand's Office of the Higher Education Commission, and Chiang Mai University that made the work in this research project possible. This funding allowed me to pursue my research interest in mechatronics and its applications on smart surgical devices. I would like to address here that much of the research work in this project was completed in collaboration with my colleagues at the Center for Mechatronic Systems and Innovation, Chiang Mai University, especially Assoc. Prof. Dr. Theeraphong Wongratanaphisan and Prof. Dr. Matthew O.T. Cole. I am grateful to Mr. Somphop Jetdumronglerd, a graduate student, who spent a great deal of effort on his work in the project. I also would like to thank members of the Motion and Control Laboratory, Department of Mechanical Engineering, Chiang Mai University, for generous assistance and fruitful discussions.

Pinyo Puangmali

# Contents

		Page
Abstract (Tha	ai)	1
Abstract (Eng	glish)	2
Executive Su	mmary	3
Acknowledge	ements	7
List of Table	s	9
List of Figure	es	10
Chapter 1 Int	roduction	12
1.1	Overview	12
1.2	Research Objectives	15
Chapter 2 Br	eakthrough Detection Technique	16
2.1	Current Measurement for Breakthrough Detection	16
2.2	Analysis of Breakthrough Detection Scheme	16
2.3	Realization of Current Sensing	18
2.4	Breakthrough Detection Algorithm	20
Chapter 3 Ex	perimental Verifications	25
3.1	Drill Prototype	25
3.2	Drilling Experiments	26
Chapter 4 Co	onclusion	32
References		34
Project Outp	ut	37
Appendix: Po	ublication	38

# **List of Tables**

		Page
Table 3.1	Thicknesses of the residual layers of acrylic remaining at the bottom	28
	of the drilled holes.	

# **List of Figures**

		Page
Fig. 1.1	Demonstrations of drilling operations using a handheld drill to	13
	drill a hole on (a) a skull and (b) a spine.	
Fig. 2.1	Model of a DC motor driving the drill chuck.	17
Fig. 2.2	Main components of current sensing and signal conditioning circuit.	18
Fig. 2.3	Current sensing and signal conditioning circuit.	19
Fig. 2.4	Typical voltage output Vo recorded while drilling a flat plate with	20
	a twist drill bit: 1) no contact between the drill bit and the object,	
	2) the peak of the first drilling step arising when the tip of the drill bit	
	begins to drill into the object, 3) half of the conical tip of the drill bit	
	penetrating into the object, 4) conical tip of the drill bit completely	
	penetrating into the object and 5) thin layer of material bent out at the	
	bottom of the hole, 6) the tip of the drill bit breaking out of the	
	object (complete breakthrough), and 7) conical tip of the drill bit	
	completely penetrating out of the object.	
Fig. 2.5	Breakthrough detection algorithm.	22
Fig. 2.6	Typical plot of the difference between $V_o$ and $\overline{V_o}$ (denoted as $V_o - \overline{V_o}$ )	23
	with indication of drilling states (see also Fig. 3). The breakthrough	
	is detected when $V_o - \overline{V_o}$ becomes lower than the secondary threshold	
	$V_{th2}$ (marked as "B").	
Fig. 3.1	Drill prototype and a piece of bone specimen.	26
Fig. 3.2	Architecture of the control system.	26
Fig. 3.3	Comparison of drilled holes on acrylic plates. Left: the holes drilled	28
	with breakthrough detection algorithm (residual thin layer of acrylic	
	at the bottom of the holes still remains as seen in white). Middle:	
	bottom of the holes drilled with breakthrough detection algorithm	

	(residual thin layer of acrylic at the bottom of the holes clearly seen	
	in white). Right: the holes drilled without breakthrough detection	
	algorithm (no residual layer of acrylic remains since the acrylic	
	plate was drilled through).	
Fig. 3.4	Typical voltage output $V_o$ recorded during drilling a hole on an acrylic	29
	plate (top) and the associated plot of $V_o - \overline{V_o}$ (bottom). A: the peak of the	
	first drilling step and B: the peak of the last drilling step that	
	the breakthrough is detected.	
Fig. 3.5	Overlaying plots of all ten drilling operations and breakthrough	29
	detection zone which the voltage differences $V_o - \overline{V_o}$ become lower	
	than $V_{th2}$ .	
Fig. 3.6	Drilling hole on the femur bone (left) and the cross-section of the	30
	hole on the bone (right).	
Fig. 3.7	Typical voltage output $V_o$ recorded during drilling a hole on a femur	31
	bone (top) and the associated plot of $V_o - \overline{V_o}$ (bottom). A: the peak of	
	the first drilling step and B: the peak of the last drilling step	
	that the breakthrough is detected	
Fig. 3.8	Cross-sections of drilling holes on four different pieces of femur	31
	bones.	

## Chapter 1

## Introduction

In bone surgery, drilling of bone without causing severe damage to tissue is a critical procedure. The process of bone drilling requires high accuracy and precision since excessive drill protrusion can cause damage to nerves, blood vessels, and nearby organs. This chapter presents the overview and objectives of research that contributes to the development of a new scheme for safe surgical bone drilling.

#### 1.1 Overview

Surgery is commonly used to treat disease and abnormalities of bones such as bone tumors, malignant bones, impaired bone joints, and disorders of tissues adjacent to the bones. The most common case is as treatment for repairing broken bones. To cure the fracture of bones, the surgeon usually performs drilling and scaffolding. However, because bones are quite rigid and difficult to cut and drill, performing such surgical procedures requires delicate skills and special tools.

In general cases of surgery, tools for drilling bones are handheld devices that are designed to operate with compressed air or electricity. Such traditional tools are portable, convenient to use, and efficient, but one of their drawbacks is that they do not have built-in safety mechanisms to ensure safe usage. The safety of drilling relies only on the perception of the surgeon. Thus, how well the surgeon can apply the tools greatly depends on his/her experience and expertise. In many critical drilling operations such as skull and spine drilling (similar to what are shown in Fig. 1.1(a) and (b)), even a small mistake can cause serious damage to blood vessels, nerves, and nearby organs. In extreme cases, this may result in paralysis or death. The surgeon must therefore be extremely careful when applying a drilling tool close to sensitive organs.





(a) (b)

Fig. 1.1 Demonstrations of drilling operations using a handheld drill to drill a hole on

(a) a skull and (b) a spine.

At present, advances in electronic and computer technology enable the development of high performance drilling equipment for bone surgery. To enhance safety, many drilling devices equipped with sensing instruments have been developed [1-7]. Several bone-breakthrough detection schemes have also been proposed over the last few decades [1-5, 7-17]. The early work of Brett and Baker on automatic breakthrough detection for precise ear surgery was carried out with an automatic lowspeed microdrill using a spherical burr [1, 2]. The major objective of this work was to automatically estimate the onset of breakthrough during stapedotomy so that the drill protrusion could be accurately controlled. The measurement of feed force and reaction torque were key to identifying the breakthrough. Although the drilling was prone to the deflection of the stapes bone under tool feed action, minimum protrusion could be achieved with the deployment of reference models used to predict the breakthrough. Later, this technique was applied with an autonomous robotic system for cochleostomy (drilling through the flexible bone tissue of the cochlear for cochlear implantation) [5]. Having the capability to identify the breakthrough from real-time sensory data of the thrust force and the drilling torque, the system could control the surgical drill tip to the required level of protrusion. Since force information is important for breakthrough detection, Ong and Bouazza-Marouf introduced a modified Kalman filter to their breakthrough detection equipment to enhance force signal processing [8]. This led to the generation of the Kalman filtered force difference between successive samples (K-FDSS) profile which enabled consistent breakthrough detection to be executed even though the drilling system with a twist drill bit was prone to the effect of inherent drilling force fluctuation.

In the field of orthopedic surgery, Allotta *et al.* reported the development of an auto-detection technique and a scheme for drill-bit penetration control [3]. In their research, the information on the drilling thrust force was used to identify states of bone drilling (with a twist drill bit). Fuzzy reasoning was adopted for controlling the feed rate of the drill such that safe orthopedic drilling operation could be performed with a specially designed hand-held tool having a force sensing unit. Subsequent work of Colla and Allotta further advanced the breakthrough detection technology by introducing wavelet analysis for signal processing [10]. Successful tests of a wavelet-based penetration control scheme demonstrated its potential applicability in preventing over travel of the drill bit during orthopedic surgery.

In order to enhance the reliability of the bone breakthrough detection, Lee and Shih proposed that feed force control should be implemented for regulating drilling torque at all times of drilling [4]. Not only thrust force information, but also drilling torque and feed rate was used together for judging the breakthrough. Using a 3-axis robotic bone drilling system, which consisted of a combined inner loop fuzzy controller for position control and outer loop PD controller for the feed unit force control, the state of penetration before the drill bit (twist drill bit) penetrated out of the bone could be identified with the threshold information of the thrust force, the trend of the drilling torque, and the feed rate of the drill.

Rather than relying on the thrust force and drilling torque information like in many other earlier proposed schemes, Osa *et al.* proposed an autonomous penetration detection scheme for cutting and drilling bones with hand-held tools [11, 12]. Since an electric drill was utilized, it was possible to use the current flowing to the motor of the drill and the rotational speed of the tool to recognize the penetration with a support vector machine (SVM) algorithm. Test results of this scheme with spherical burr demonstrated that, not only thrust force and drilling torque, but also current and drill speed can be important indicators for recognizing states of bone penetration.

For most of the previously proposed drilling systems, real-time feed-force information is required for breakthrough detection. Thus, the installation of a force sensing instrument in the drilling system is essential [1], [3], [4], [8-10], [13-17]. In our research, the study of drilling mechanics leads to the proposition of an alternative scheme developed for bone drilling procedures that use a twist drill bit (the most widely used drilling tool in orthopedic surgery). This new scheme requires neither the installation of a force sensor nor the measurement of feed force. The novelty of the scheme is based on the integration of three key elements: current sensing, stepwise drilling, and hysteresis thresholding. A prototype of a drilling tool equipped with electronics for current sensing and signal conditioning has been shown to perform successful drilling while achieving effective breakthrough detection without force measurement.

### 1.2 Research Objectives

Since the capability of detecting breakthrough precisely is an important key to safe surgical drilling of bone, this project was created for contributing the development of a new breakthrough detection scheme. The objectives of the project were:

- To find an effective means for bone breakthrough detection in bone drilling operation.
- To develop a breakthrough detection system that can perform bone breakthrough detection with high reliability.
- To develop a bone drilling tool that can be used to carry out precise surgical procedures.

In this chapter, the overview of breakthrough detection techniques and objectives of research that contributes to the development of a new scheme for safe surgical bone drilling is presented. Such a new scheme was developed based on the analysis of drilling operation. More details on the analysis of drilling characteristics will be described in the next chapter.

# Chapter 2

# **Breakthrough Detection Technique**

There are various techniques that have been tested and verified for practical bone drilling procedures. Current measurement technique is considered one of the key techniques that can be applied for breakthrough detection. This chapter provide details of this technique and the analysis of its applicability in surgical drilling.

## 2.1 Current Measurement for Breakthrough Detection

According to the physical operation of an electric drill, an increment of drilling torque load while drilling causes the motor driving the drill spindle to consume more current. However, when the breakthrough is occurring, the torque load declines, causing the current to reduce simultaneously. In principle, this phenomenon allows breakthrough to be detected based on the monitoring only of the motor current. A simple indicator for identifying the breakthrough involves a threshold value which can be determined slightly higher than the amount of current at no load. When the current flowing to the motor diminishes to such a value (usually during the occurrence of the breakthrough), the breakthrough is detected.

Breakthrough detection based on current measurement is considered an effective approach since, in typical set-ups, the current responds to torque load change very quickly. The measurement of current is also simple since it can be carried out without need of modifying the structure of the drill to install a sensor. Instead, it can be realized by connecting the drill with a current sensing circuit.

## 2.2 Analysis of Breakthrough Detection Scheme

To analyze the motor current behavior, a model of a direct current (DC) motor driving the drill chuck with direct transmission of power (without gearing) is considered, as shown in Fig. 2.1. This model can be expressed mathematically as the following governing equations [18]:

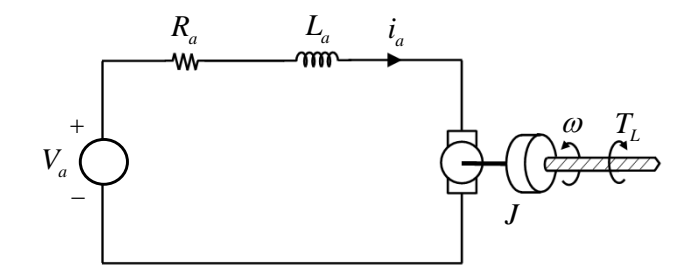


Fig. 2.1 Model of a DC motor driving the drill chuck.

$$\frac{d}{dt}i_a = -\frac{R_a}{L_a}i_a - \frac{k_v}{L_a}\omega + \frac{V_a}{L_a} \tag{2.1}$$

$$\frac{d}{dt}\omega = \frac{k_t}{J}i_a - \frac{b_m}{J}\omega - \frac{1}{J}T_L,$$
(2.2)

where  $i_a$  represents current flowing through the armature winding of the motor,  $R_a$ ,  $L_a$ , and  $V_a$  are resistance, inductance, and voltage of the armature winding,  $k_v$  is back electromotive force (emf) constant,  $\omega$  is rotational speed of the drill,  $k_t$  is torque constant of the motor, J is effective moment of inertia of the rotating parts,  $b_m$  is viscous friction coefficient of the motor, and  $T_L$  is torque load caused by drilling. Equations (2.1) and (2.2) may be expressed in the Laplace domain as

$$I_{a}(s) = \frac{1}{L_{a}s + R_{a}} (V_{a}(s) - k_{\nu}\Omega(s))$$
 (2.3)

$$\Omega(s) = \frac{1}{J_s + b_m} (k_t I_a(s) - T_L(s)), \tag{2.4}$$

where  $I_a(s)$ ,  $V_a(s)$ ,  $\Omega(s)$ , and  $T_L(s)$  represent the Laplace transforms of  $i_a$ ,  $V_a$ ,  $\omega$ , and  $T_L$  respectively. By substituting (2.4) into (2.3) and rearranging, an expression for  $I_a(s)$  can be determined as

$$I_{a}(s) = \frac{Js + b_{m}}{L_{a}Js^{2} + (L_{a}b_{m} + R_{a}J)s + (R_{a}b_{m} + k_{v}k_{t})}V_{a}(s) + \frac{k_{v}}{L_{c}Js^{2} + (L_{a}b_{m} + R_{a}J)s + (R_{a}b_{m} + k_{v}k_{t})}T_{L}(s).$$

$$(2.5)$$

Equation (2.5) indicates that current change occurs in relation to the voltage of the armature winding  $V_a(s)$  and torque load  $T_L(s)$ . If voltage  $V_a$  is regulated to a constant

value by the voltage-source power supply, changes of current will depend only on the torque load. When the drill experiences no load, the current is usually steady at a constant value (no-load current value). Afterward, when the drill bit progresses into the bone, the torque load acts at the tip of the drill causing the current to increase. Finally, when the drill is breaking through the bone, torque load will significantly diminish, causing the current to drop. Significant reduction of current therefore indicates the occurrence of the breakthrough.

### 2.3 Realization of Current Sensing

In practice, the level of current flowing through the motor may be determined by the use of a sense resistor. Figure 2.2 shows a sense resistor connected in series with the motor. The voltage across this sense resistor is the sensing signal which is processed by a signal conditioning circuit comprising an isolation amplifier, a differential amplifier, and an instrumentation amplifier. The isolation amplifier associated with input filter components is used to perform initial filtering for suppressing high-frequency noise while providing electrical isolation between the power line and other parts of the signal conditioning circuit. The output of the isolation amplifier is processed by a unity-gain differential amplifier associated with capacitors for further noise filtering. These filtering components are included for suppressing commutation ripple before the signal is offset and amplified to the required level by an instrumentation amplifier. Figure 2.3 shows the schematic of the circuit. In the Laplace domain, the voltage across the sense resistor  $V_{sr}(s)$  is an analog signal whose magnitude varies with the amount of current flowing through the motor according to

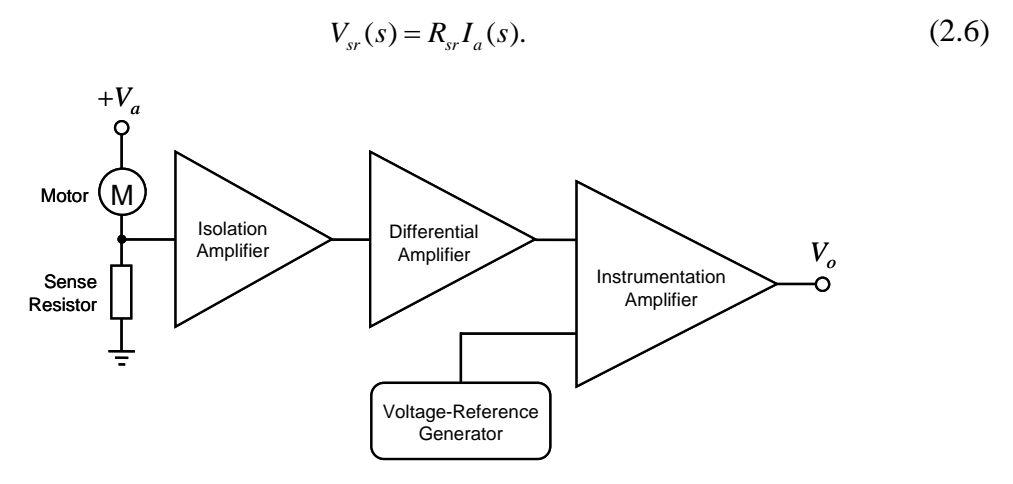


Fig. 2.2 Main components of current sensing and signal conditioning circuit.

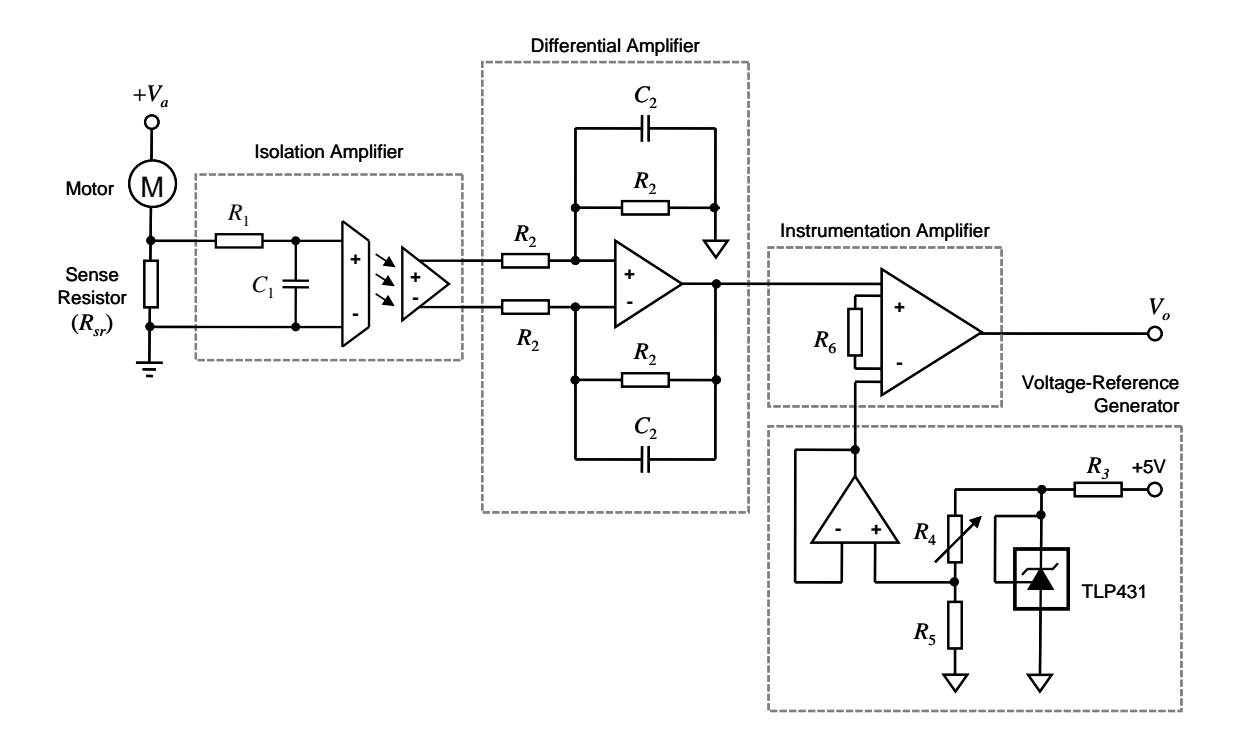


Fig. 2.3 Current sensing and signal conditioning circuit.

The analog signal  $V_{sr}(s)$  is filtered, amplified, and offset by the signal conditioning circuit to obtain the voltage output  $V_o$  which is given by

$$V_o(s) = k_2[k_1 V_{sr}(s) - V_{ref}(s)]. (2.7)$$

In this equation,  $k_1$  and  $k_2$  are gains of the isolation amplifier and the instrumentation amplifier respectively.  $V_{ref}(s)$  is the constant reference voltage obtained from a precision voltage reference generator. The voltage from this device is used to adjust the offset of  $V_{sr}(s)$  after high frequency noise is filtered out. Substituting  $V_{sr}(s)$  in (2.7), we obtain

$$\begin{split} V_{o}(s) &= k_{2}[k_{1}R_{sr}I_{a}(s) - V_{ref}] \\ &= k_{2}k_{1}R_{sr}I_{a}(s) - k_{2}V_{ref} \\ &= \frac{k_{2}k_{1}R_{sr}Js + k_{2}k_{1}R_{sr}b_{m}}{L_{a}Js^{2} + (L_{a}b_{m} + R_{a}J)s + (R_{a}b_{m} + k_{v}k_{t})}V_{a}(s) \\ &+ \frac{k_{v}k_{2}k_{1}R_{sr}}{L_{a}Js^{2} + (L_{a}b_{m} + R_{a}J)s + (R_{a}b_{m} + k_{v}k_{t})}T_{L}(s) - k_{2}V_{ref}. \end{split}$$

It should be noted that, transient effects from electronic components (including filters and amplifiers) are neglected here since their responses are much faster than that of the motor. In (2.8), if  $V_{ref}(s)$  is set such that the magnitudes of the first and the last terms become close to each other in steady state, the voltage output  $V_o(s)$  can be simply

determined as

$$V_o(s) \approx \frac{k_v k_2 k_1 R_{sr}}{L_a J s^2 + (L_a b_m + R_a J) s + (R_a b_m + k_v k_t)} T_L(s). \tag{2.9}$$

For typical small-sized low-inertia DC motors, the transfer function obtained from (2.9) behaves as a low-pass filter having high bandwidth due to the existence of fast system poles. This property gives good characteristics for measuring transient features of the torque load profile. The variation in voltage output  $V_o$  for a typical drilling torque load, produced when the drill bit penetrates into an object in short quick steps until the breakthrough is reached, is shown in Fig. 2.4. It can be seen that the voltage output responds to the changing torque load very quickly to produce a clear peak each time the drill is advanced. This behavior can be exploited for accurate detection of the breakthrough.

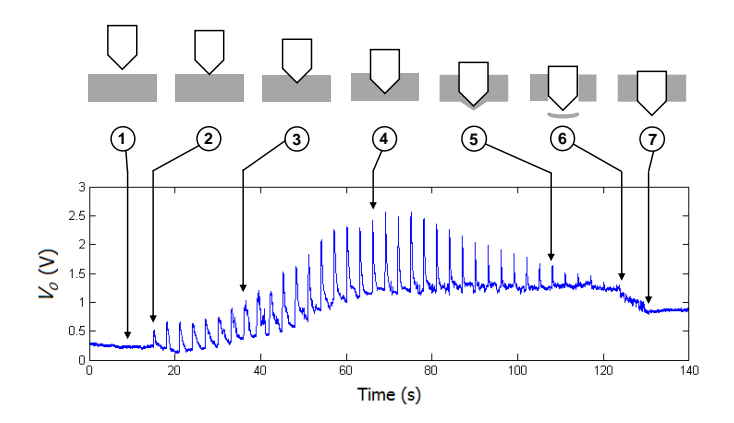


Fig. 2.4 Typical voltage output  $V_o$  recorded while drilling a flat plate with a twist drill bit: 1) no contact between the drill bit and the object, 2) the peak of the first drilling step arising when the tip of the drill bit begins to drill into the object, 3) half of the conical tip of the drill bit penetrating into the object, 4) conical tip of the drill bit completely penetrating into the object and 5) thin layer of material bent out at the bottom of the hole, 6) the tip of the drill bit breaking out of the object (complete breakthrough), and 7) conical tip of the drill bit completely penetrating out of the object.

### 2.4 Breakthrough Detection Algorithm

To identify breakthrough, the magnitude of the voltage output  $V_o$  is sampled and the breakthrough detection algorithm applied. This algorithm is designed to detect the

breakthrough when executing stepwise drilling. This drilling procedure involves a controlled motion of the drill such that a sub-millimeter increase in drilling depth occurs for each step. Several successive drilling steps are carried out until the breakthrough occurs. Because the drill movement is stepwise, drilling torque load is approximately periodic (see the plot in Fig. 2.4). While executing each drilling step, there is a sharp peak in the torque load. Each peak also produces a peak in the voltage output signal. Several steps of drilling are executed until the tip of the drill is about to break out of the object being drilled. The magnitude of the peak then declines. By applying an algorithm based on the measurement of the peaks, the breakthrough can therefore be detected when the magnitude of the peak diminishes to zero.

In practice, contamination of noise in the sampled signal occurs. An averaging technique for noise reduction is therefore applied during the process of breakthrough identification. As shown in Fig. 2.5, n initial values of  $V_o$  are recorded prior to feeding the drill toward the object. The average of these initial values represents the minimal value of  $V_o$ , denoted as  $\overline{V}_o$ . After recording these values, the drill is fed toward the object with a small increase in drilling depth over a short period of time ( $t_{\text{feed}}$ ). In the initial drilling phase, if the tip of the drill bit does not contact with the object, the torque load remains zero. Short stepwise feeds are repeated (as long as the drill does not move beyond a predefined allowable safety range) until the tip of the drill bit comes into contact with the object. The time period for each repetition of a stepwise feed ( $t_{repeat}$ ) is set sufficiently long to complete a small drilling step ( $t_{repeat} >> t_{feed}$ ) that is required to cut and remove material out of the drilled hole. When the lips (cutting edges at the tip) of the drill bit begin cutting into the object, the torque load rapidly increases causing  $V_o$ to increase to a peak value and then decline (see the plot in Fig. 2.4). For the advantage of noise immunity, an average is also calculated to estimate the peak of the signal based on the m highest sampled values of  $V_o$  recorded during advancement of the drill. This average is denoted as  $V_o$ . The value of  $V_o$  is compared to the averaged initial value,  $\overline{V_o}$ . If the difference between these two values is higher than the primary threshold value  $(V_0 - \overline{V_0} > V_{th1})$ , the drill is recognized to be in the main drilling phase (see Fig. 2.6). Based on experimental verifications, a practical value of the primary threshold  $V_{th1}$  can be determined as the voltage difference  $V_{o} - \overline{V_{o}}$  when half of the conical tip of the drill bit penetrates into the object. When the penetration is deeper than half of the conical tip

of the drill bit, it is considered to be in the main drilling phase. Stepwise drilling motion then continues while the algorithm keeps monitoring the voltage difference  $V_o - \overline{V_o}$ . The voltage difference  $V_o - \overline{V_o}$  usually remains higher than  $V_{th1}$  until the breakthrough starts to occur. In the breakthrough phase, the voltage difference  $V_o - \overline{V_o}$  reduces successively. If the difference between  $V_o$  and  $\overline{V_o}$  drops to zero, the complete breakthrough is reached. However, another threshold—the secondary threshold  $(V_{th2})$ —is set to recognize the early state of the breakthrough. If the voltage difference  $V_o - \overline{V_o}$  becomes less than this secondary threshold value  $(V_o - \overline{V_o} < V_{th2})$ , the breakthrough state is detected, as shown in Fig. 2.6.

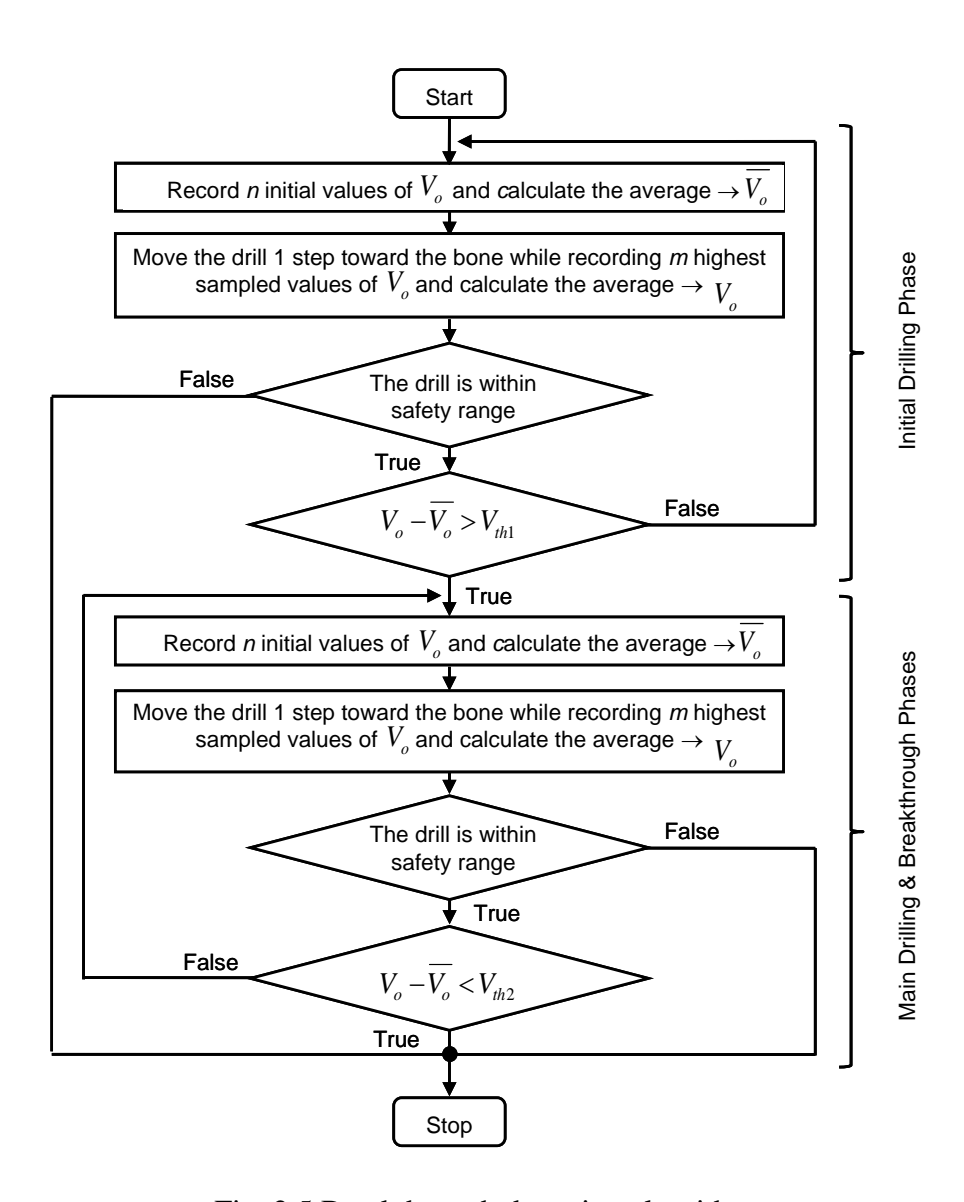


Fig. 2.5 Breakthrough detection algorithm.

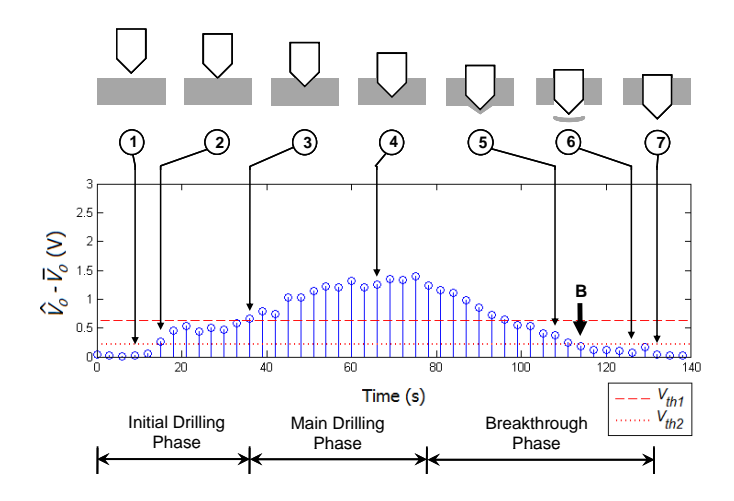


Fig. 2.6 Typical plot of the difference between  $V_o$  and  $\overline{V_o}$  (denoted as  $V_o - \overline{V_o}$ ) with indication of drilling states (see also Fig. 2.4). The breakthrough is detected when  $V_o - \overline{V_o}$  becomes lower than the secondary threshold  $V_{th2}$  (marked as "B").

To negate the measurement uncertainty that may lead to fault breakthrough detection in practice,  $V_{th2}$  should be set slightly higher than the upper deviation of the voltage differences  $V_o - \overline{V_o}$  when the drill has no drilling load. Higher value of  $V_{th2}$  may be set for early detection of the breakthrough, allowing a safety margin to prevent over drilling in critical surgical procedures. It should be noted that, according to the hysteresis thresholding principle,  $V_{th2}$  and  $V_{th1}$  form the lower and upper thresholds for breakthrough state recognition with uncertainty immunity. Since the voltage differences  $V_o - \overline{V_o}$  can fluctuate due to electrical noise, mechanical vibration, and inhomogeneity of bone, having large difference band between  $V_{th1}$  and  $V_{th2}$  by keeping  $V_{th2}$  low is essential for maintaining high reliability of breakthrough detection. In practice, the achievable difference band is dependent on the properties of the drilled material.

In this chapter, the current measurement principle for breakthrough detection and the analysis of breakthrough detection scheme are presented. A realization technique of effective current sensing using a specially designed electronic circuit is subsequently described. Such an electronic circuit is an important part of the breakthrough detection system which operates based on breakthrough detection

algorithm. In the next chapter, the integration of electronic devices with other hardware of a drill prototype will further be described. Details of the experimental verification of the drill prototype will also be provided.

# Chapter 3

# **Experimental Verifications**

To verify the effectiveness of the breakthrough detection scheme, experimental tests were conducted with a drill prototype that operates based on breakthrough detection algorithm. This chapter describes the drill prototype and results of drilling experiments.

## 3.1 Drill Prototype

The breakthrough detection scheme was tested using a drill prototype which is composed of an electric drill with a twist drill bit, associated electronics, and a drill stand. Figure 3.1 depicts this prototype with a piece of bone specimen clamped in place by a bench vice. The architecture of the control system associated with this prototype is shown in Fig. 3.2. The main component of the drill is a permanent magnet DC motor which is coupled directly with the drill chuck without speed control. It is installed on a 1-mm-pitch ball-screw linear actuator driven by a DC servo motor (Faulhaber Schonaich 3557K024CS). To perform precise control of the drill feed motion, a proportional-integral-derivative (PID) control algorithm is implemented in a 32-bit microcontroller (STM32F407VG) combined with an H-bridge motor driver circuit. This motion control algorithm was tuned to provide an overdamped response with rise time of 24 ms. Operating at a sampling frequency of 1 kHz, the microcontroller uses its internal 12-bit analog-to-digital converter for sampling the analog signal from the breakthrough detection circuit such that, as soon as the occurrence of the breakthrough is detected, it can control the drill bit to move out of the drilled hole.

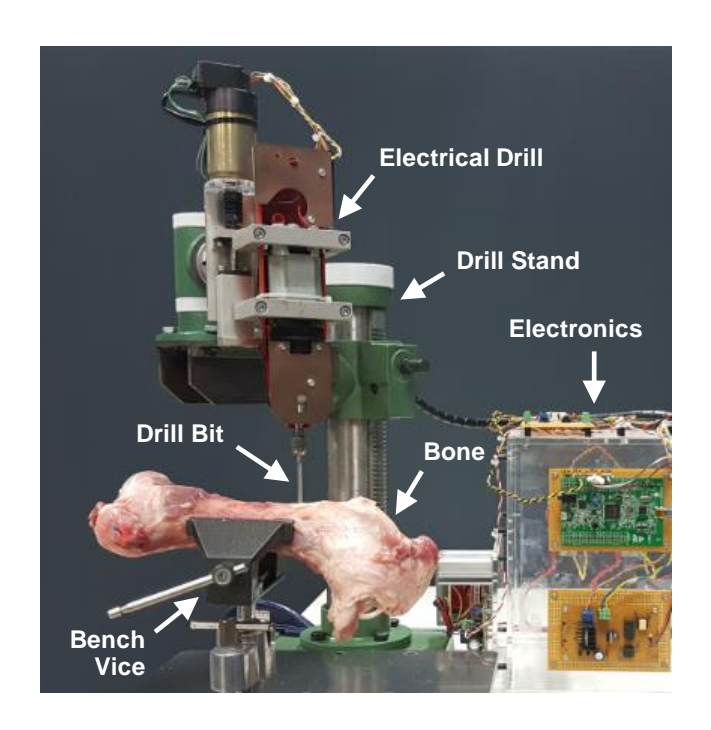


Fig. 3.1 Drill prototype and a piece of bone specimen.

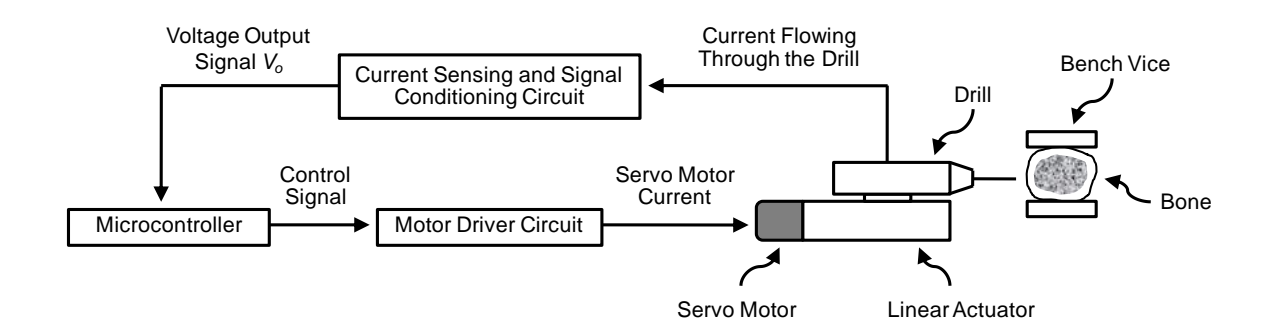


Fig. 3.2 Architecture of the control system.

### 3.2 Drilling Experiments

Two drilling experiments were conducted with the drill prototype to verify the breakthrough detection and control algorithms. The first experiment was conducted with acrylic plates. The other experiment was conducted with porcine bones. To carry out these experiments, a 3.2-mm twist drill bit was used. The drill was controlled to move step-by-step with a step size of 0.1 mm and time period of 3 s while the drill chuck rotated at a speed of 7950 rpm (no-load speed). Note that step size is one of the key parameters for successful breakthrough detection since it affects both detectability and

precision of the breakthrough detection scheme. Small step size is mostly desirable since it increases the positional precision. However, if the step size is too small, the detectability of breakthrough detection and immunity to uncertainty will be poor due to reduced current peaks. On the contrary, if step size is big, the detectability is high but the precision is low due to reduced motion control resolution. Depending on the application, different step sizes may be set based on target criterion for the tradeoff between detectability and precision. Equipment associated with these two experiments is as shown in Fig. 3.1. Details and results of each experiment are described as follows:

1) Drilling acrylic plates. Three pieces of 3-mm-thickness transparent acrylic plates were used as specimens. The first two pieces were used for breakthrough detection tests. Each specimen was clamped on a bench vice while drilling was controlled according to the breakthrough detection algorithm shown in Fig. 2.5. The third piece of specimen was used for drilling holes through without breakthrough detection. In breakthrough detection tests, the values of  $V_{o}$  and  $\overline{V_{o}}$  were individually calculated from 5 sampled values (n = m = 5). The primary threshold  $V_{th1}$  was set to 0.6 volts ( $V_{th1} = 0.6$ ) which is approximately equal to the voltage difference  $V_o - \overline{V_o}$  observed when half of the conical tip of the drill bit penetrated into the acrylic plates. The secondary threshold  $V_{th2}$  was set to 0.2 volts ( $V_{th2} = 0.2$ ) enabling early detection of the breakthrough to be carried out. Note that the value of this secondary threshold is higher than the upper deviation of the voltage differences  $V_{o} - \overline{V_{o}}$  when the drill has no drilling load as described in Section 2.4. When the breakthrough occurred, the drill bit was removed from the drilled hole immediately. Only a small residual layer of acrylic remained at the bottom of the hole. The drilling operation was repeated for ten drilled holes (five holes on each acrylic plate). The holes drilled with the breakthrough detection scheme compared with holes drilled without the breakthrough scheme are shown in Fig. 3.3. Table 3.1 shows the thicknesses of the residual layer of acrylic obtained from each time of drilling. The average is approximately 0.19 mm. This result shows that slightly early detection before the occurrence of complete breakthrough is precisely carried out with the thresholds specified based on the described criterion.



Fig. 3.3 Comparison of drilled holes on acrylic plates. Left: the holes drilled with breakthrough detection algorithm (residual thin layer of acrylic at the bottom of the holes still remains as seen in white). Middle: bottom of the holes drilled with breakthrough detection algorithm (residual thin layer of acrylic at the bottom of the holes clearly seen in white). Right: the holes drilled without breakthrough detection algorithm (no residual layer of acrylic remains since the acrylic plate was drilled through).

Table 3.1 Thicknesses of the residual layers of acrylic remaining at the bottom of the drilled holes.

Hole No.	Thickness (mm)	Hole No.	Thickness (mm)
1	0.17	6	0.21
2	0.17	7	0.22
3	0.18	8	0.22
4	0.19	9	0.22
5	0.19	10	0.17
Average		0.	19
Standard Deviation		0.	02

In Fig. 3.4, a typical voltage output  $V_o$  and voltage difference  $V_o - \overline{V_o}$  recorded throughout the operation of drilling is shown. As can be seen, after several steps of drilling, the peak voltage value of each drilling step declined. Drilling was terminated when the voltage difference  $V_o - \overline{V_o}$  dropped below the secondary threshold  $V_{th2}$ . Thirty-five drilling steps, equivalent to the travel distance of approximately 3.5 mm, was executed before the breakthrough was detected. This exceeds the thickness of the acrylic plate (3.0 mm) because the residual layer of acrylic was bent out at the bottom of the hole before complete breakthrough occurred (see Figs. 2.4 and 2.6). Fig. 3.5

illustrates overlaying plots of all ten drilling operations showing the consistency of the voltage signals and breakthrough detection zone in which the voltage differences  $V_o - \overline{V_o}$  become lower than  $V_{th2}$ . It is clear that, after 33–35 drilling steps, the breakthrough was detected in this zone. The deviation of breakthrough detection is therefore less than 3 drilling steps or, in other word, within 0.3 mm (step size = 0.1 mm).

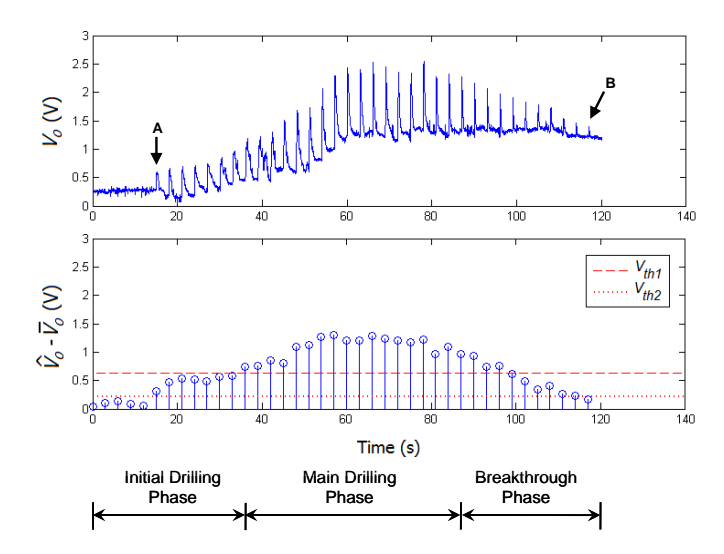


Fig. 3.4 Typical voltage output  $V_o$  recorded during drilling a hole on an acrylic plate (top) and the associated plot of  $V_o - \overline{V_o}$  (bottom). A: the peak of the first drilling step and B: the peak of the last drilling step that the breakthrough is detected.

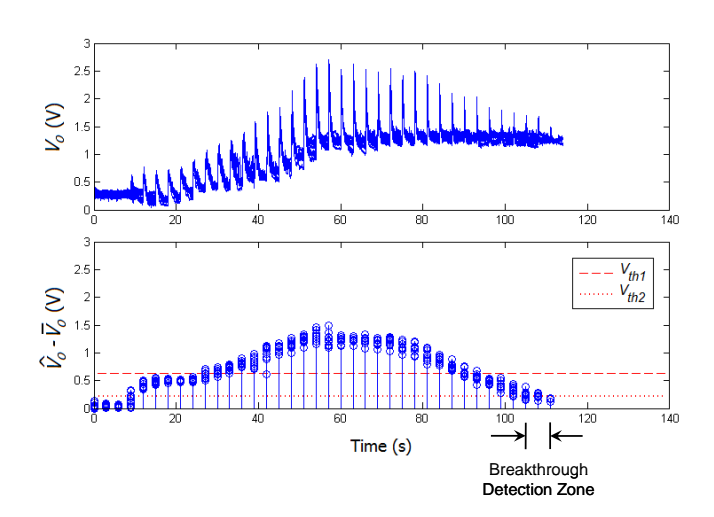


Fig. 3.5 Overlaying plots of all ten drilling operations and breakthrough detection zone which the voltage differences  $V_o - \overline{V_o}$  become lower than  $V_{th2}$ .

2) Drilling porcine bones. Four pieces of femur bones were used as specimens in the second experiment. Every specimen has two distinct bone layers: cortical bone layer (the outer hard layer) and cancellous bone layer (the inner soft porous layer). While performing drilling, each bone was clamped in place. The same settings for all parameters including the spindle speed were applied in this case as in the previous experiment. In this experiment, the objective was to detect the breakthrough when the drill bit started to penetrate out of the cortical bone to the inner porous layer of the cancellous bone. After several steps of drilling, the breakthrough was successfully detected. Figure 3.6 shows a typical drilled hole and the bone cross-section. As can be seen from the figure, drilling stopped at the boundary of the cortical and cancellous bone layers. Very little damage to the cancellous bone was caused. The records of voltage output  $V_o$  and the voltage difference  $V_o - \overline{V_o}$  associated with this experiment are shown in Fig. 3.7. Compared to the case of drilling acrylic plates, the response of the measurement signal in this case has a more irregular pattern. This was mainly due to the inhomogeneous structure of the bone material. In Fig. 3.8, the cross-sections of drilled holes on four different pieces of bones are shown. It is clear that only little damage was caused to the cancellous bones because the conical tip of the drill bit travelled only slightly beyond the boundary of the cortical and cancellous bones and was stopped before complete cuts of the cortical bones by the cutting edges at the tip of the drill bit were made.



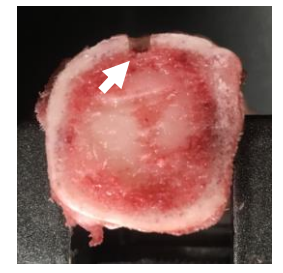


Fig. 3.6 Drilling hole on the femur bone (left) and the cross-section of the hole on the bone (right).

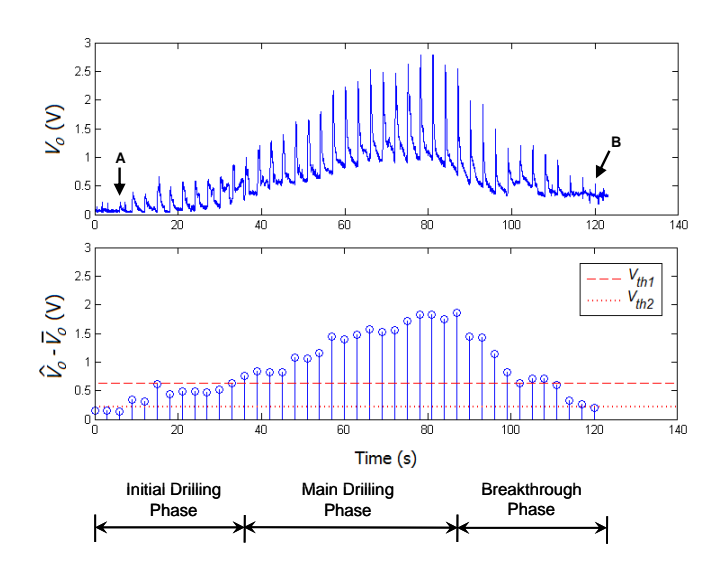


Fig. 3.7 Typical voltage output  $V_o$  recorded during drilling a hole on a femur bone (top) and the associated plot of  $V_o - \overline{V_o}$  (bottom). A: the peak of the first drilling step and B: the peak of the last drilling step that the breakthrough is detected.



Fig. 3.8 Cross-sections of drilling holes on four different pieces of femur bones.

This chapter describes details of the drill prototype used to conduct experimental verification of the breakthrough detection scheme. Results of drilling experiments are the evidences of successful breakthrough detection while performing bone drilling operation. Although these results clearly show the possibility of performing breakthrough detection, there are some limitations that requires further research as will be discussed in the next chapter.

# **Chapter 4**

## Conclusion

In this research, the combination of three key techniques is proposed for breakthrough detection in bone drilling procedures: 1) measurement of current flowing though the motor of the electric drill using a sense resistor, 2) stepwise drilling action controlled by a microcontroller, and 3) hysteresis thresholding for breakthrough detection with uncertainty immunity. The measurement of current can be performed effectively by applying a sense resistor with specially designed signal conditioning circuit, which is composed of an isolation amplifier, a unity-gain differential amplifier with input filter components, and an instrumentation amplifier. With the stepwise drilling action, there is a peak in the measurement signal at each step of drilling. By monitoring the peak, the breakthrough can be identified since, when the breakthrough begins to occur, the peaks at successive drilling steps decline. If the peak declines below threshold values according to the hysteresis thresholding principle, the drilling process is terminated and the drill bit removed from the drilled hole. This drilling procedure allows safe drilling to be executed. For real surgery, severe damage of soft tissue underneath the hard layer of bone can be prevented.

A number of drilling experiments with acrylic plates and porcine bones showed that threshold values are important parameters for successful breakthrough detection. When they are properly specified, the breakthrough can be effectively detected in real-time with the proposed scheme. However, the main limitation of this scheme is that tuning of detection parameters for specific bone types and drilling conditions associated with different drill bit sizes and shapes is required. Initially, this would be done based on empirical data from calibration testing on sample bone specimens. Over time, compiling a large set of test results will allow more general tuning rules to be established. Moreover, further investigations on the effects of spindle speed, stiffness of the drill stand, and stiffness of the drilled object itself are also required since they influence threshold setting. Although twist drill bits are commonly used, other types of

cutting tools for drilling such as spherical burrs, round-nose end mills, and square end mills should also be tested for evaluation and further development of the breakthrough detection scheme.

## References

- [1] Brett PN, Baker DA, Reyes L, Blanshard J. An automatic technique for microdrilling a stapedotomy in the flexible stapes footplate. Proceedings of the Institution of Mechanical Engineers, Part H: Journal of Engineering in Medicine. 1995;209(4):255-62.
- [2] Baker D, Brett PN, Griffiths MV, Reyes L. A mechatronic drilling tool for ear surgery: A case study of some design characteristics. Mechatronics. 1996 1;6(4):461-77.
- [3] Allotta B, Giacalone G, Rinaldi L. A hand-held drilling tool for orthopedic surgery. IEEE/ASME Transactions on Mechatronics. 1997;2(4):218-29.
- [4] Lee WY, Shih CL. Control and breakthrough detection of a three-axis robotic bone drilling system. Mechatronics. 2006;16(2):73-84.
- [5] Brett PN, Taylor RP, Proops D, Coulson C, Reid A, Griffiths MV. A surgical robot for cochleostomy. In the Proceedings of the 29th Annual International Conference of the IEEE EMBS. 2007;1229-32.
- [6] Kotev V, Boiadjiev G, Kawasaki H, Mouri T, Delchev K, Boiadjiev T. Design of a hand-held robotized module for bone drilling and cutting in orthopedic surgery. Design of a hand-held robotized module for bone drilling and cutting in orthopedic surgery. In the Proceedings of the IEEE/SICE International Symposium on System Integration (SII). 2012;504-9.
- [7] Díaz I, Gil JJ, Louredo M. Bone drilling methodology and tool based on position measurements. Computer methods and programs in biomedicine. 2013;112(2):284-92.
- [8] Ong FR, Bouazza-Marouf K. The detection of drill bit break-through for the enhancement of safety in mechatronic assisted orthopaedic drilling. Mechatronics. 1999;9(6):565-88.

- [9] Allotta B, Belmonte F, Bosio L, Dario P. Study on a mechatronic tool for drilling in the osteosynthesis of long bones: tool/bone interaction, modeling and experiments. Mechatronics. 1996;6(4):447-59.
- [10] Colla V, Allotta B. Wavelet-based control of penetration in a mechatronic drill for orthopaedic surgery. In the Proceedings of the IEEE International Conference on Robotics and Automation (ICRA 1998). 1998;711-6.
- [11] Osa T, Abawi CF, Sugita N, Chikuda H, Sugita S, Ito H, Moro T, Takatori Y, Tanaka S, Mitsuishi M. Autonomous penetration detection for bone cutting tool using demonstration-based learning. In the Proceedings of the IEEE International Conference on Robotics and Automation (ICRA 2014). 2014;290-6.
- Osa T, Abawi CF, Sugita N, Chikuda H, Sugita S, Tanaka T, Oshima H, Moro T, Tanaka S, Mitsuishi M. Hand-held bone cutting tool with autonomous penetration detection for spinal surgery. IEEE/ASME Trans. Mechatron. 2015;20(6):3018-27.
- [13] Hu Y, Jin H, Zhang L, Zhang P, Zhang J. State recognition of pedicle drilling with force sensing in a robotic spinal surgical system. IEEE/ASME Transactions on Mechatronics. 2014;19(1):357-65.
- [14] Jiang Z, Sun Y, Zhao S, Hu Y, Zhang J. A model of vertebral motion and key point recognition of drilling with force in robot-assisted spinal surgery. In the Proceedings of the IEEE/RSJ International Conference on Intelligent Robots and Systems (IROS 2017). 2017;6455-62.
- [15] Qi L, Meng MQ. Real-time break-through detection of bone drilling based on wavelet transform for robot assisted orthopedic surgery. In the Proceedings of the IEEE International Conference on Robotics and Biomimetics (ROBIO 2014). 2014;601-6.
- [16] Sun Y, Jin H, Hu Y, Zhang P, Zhang J. State recognition of bone drilling with audio signal in robotic orthopedics surgery system. In the Proceedings of the IEEE/RSJ International Conference on Intelligent Robots and Systems (IROS 2014). 2014;3503-8.
- [17] Jin H, Hu Y, Deng Z, Zhang P, Song Z, Zhang J. Model-based state recognition of bone drilling with robotic orthopedic surgery system. In the

- Proceedings of the IEEE International Conference on Robotics and Automation (ICRA 2014). 2014;3538-43.
- [18] Kuo BC, Golnaraghi F. Automatic Control Systems. 8th ed. New York: John Wiley & Sons; 2003.

### **Project Output**

#### **Journal Publication**

Puangmali, P., Jetdumronglerd, S., Wongratanaphisan, T. and Cole, M.O., "Sensorless stepwise breakthrough detection technique for safe surgical drilling of bone." Mechatronics 65 (2020): 102306. (Q1, Impact Factor 2.992)

# Appendix Publication



Contents lists available at ScienceDirect

#### Mechatronics

journal homepage: www.elsevier.com/locate/mechatronics



## Sensorless stepwise breakthrough detection technique for safe surgical drilling of bone



Pinyo Puangmali<sup>a,b,\*</sup>, Somphop Jetdumronglerd<sup>a</sup>, Theeraphong Wongratanaphisan<sup>a,b</sup>, Matthew O.T. Cole<sup>a,b</sup>

<sup>a</sup> Department of Mechanical Engineering, Faculty of Engineering, Chiang Mai University, 239 Huay Kaew Rd., Muang District, Chiang Mai 50200, Thailand

#### ARTICLE INFO

#### Keywords: Breakthrough detection Breakout detection Penetration detection Penetration control Surgical drilling

#### ABSTRACT

In bone surgery, drilling of bone without causing severe damage to tissue is a critical procedure. Particularly for skull, spine, and special kinds of orthopedic surgeries, the process of bone drilling requires high accuracy and precision since excessive drill protrusion can cause damage to nerves, blood vessels, and nearby organs. To enhance safety of drilling, a new breakthrough detection technique that does not require the installation of a sensor for force or torque measurement is proposed. This technique relies only on the measurement of current flowing through the motor of an electric drill to monitor drilling progress. By measuring the amount of current while executing stepwise drilling and applying a hysteresis thresholding algorithm, the breakthrough event can be effectively identified in real-time. Experimental tests of a drill prototype utilizing this scheme showed that breakthrough could be consistently detected. This prevents over drilling, enabling reliable drilling operation which can minimize tissue damage.

#### 1. Introduction

Surgery is commonly used to treat disease and abnormalities of bones such as bone tumors, malignant bones, impaired bone joints, and disorders of tissues adjacent to the bones. The most common case is as treatment for repairing broken bones. To cure the fracture of bones, the surgeon usually performs drilling and scaffolding. However, because bones are quite rigid and difficult to cut and drill, performing such surgical procedures requires delicate skills and special tools.

In general cases of surgery, tools for drilling bones are handheld devices that are designed to operate with compressed air or electricity. Such traditional tools are portable, convenient to use, and efficient, but one of their drawbacks is that they do not have built-in safety mechanisms to ensure safe usage. The safety of drilling relies only on the perception of the surgeon. Thus, how well the surgeon can apply the tools greatly depends on his/her experience and expertise. In many critical drilling operations such as skull and spine drilling, even a small mistake can cause serious damage to blood vessels, nerves, and nearby organs. In extreme cases, this may result in paralysis or death. The surgeon must therefore be extremely careful when applying a drilling tool close to sensitive organs.

E-mail address: pinyo@dome.eng.cmu.ac.th (P. Puangmali).

At present, advances in electronic and computer technology enable the development of high performance drilling equipment for bone surgery. To enhance safety, many drilling devices equipped with sensing instruments have been developed [1–7]. Several bone-breakthrough detection schemes have also been proposed over the last few decades [1– 5,7–17]. The early work of Brett and Baker on automatic breakthrough detection for precise ear surgery was carried out with an automatic lowspeed microdrill using a spherical burr [1,2]. The major objective of this work was to automatically estimate the onset of breakthrough during stapedotomy so that the drill protrusion could be accurately controlled. The measurement of feed force and reaction torque were key to identifying the breakthrough. Although the drilling was prone to the deflection of the stapes bone under tool feed action, minimum protrusion could be achieved with the deployment of reference models used to predict the breakthrough. Later, this technique was applied with an autonomous robotic system for cochleostomy (drilling through the flexible bone tissue of the cochlear for cochlear implantation) [5]. Having the capability to identify the breakthrough from real-time sensory data of the thrust force and the drilling torque, the system could control the surgical drill tip to the required level of protrusion. Since force information is important for breakthrough detection, Ong and Bouazza-Marouf introduced a modified Kalman filter to their breakthrough detection equipment to enhance force signal processing [8]. This led to the generation of the Kalman filtered force difference between successive samples (K-FDSS) profile which enabled consistent breakthrough detection to be executed even though the drilling system with a twist drill bit was prone to the effect of inherent drilling force fluctuation.

<sup>&</sup>lt;sup>b</sup> Center for Mechatronic Systems and Innovation, Chiang Mai University, 239 Huay Kaew Rd., Muang District, Chiang Mai 50200, Thailand

<sup>\*</sup> Corresponding author at: Department of Mechanical Engineering, Faculty of Engineering, Chiang Mai University, 239 Huay Kaew Rd., Muang District, Chiang Mai 50200, Thailand.

In the field of orthopedic surgery, Allotta et al. reported the development of an auto-detection technique and a scheme for drill-bit penetration control [3]. In their research, the information on the drilling thrust force was used to identify states of bone drilling (with a twist drill bit). Fuzzy reasoning was adopted for controlling the feed rate of the drill such that safe orthopedic drilling operation could be performed with a specially designed hand-held tool having a force sensing unit. Subsequent work of Colla and Allotta further advanced the breakthrough detection technology by introducing wavelet analysis for signal processing [10]. Successful tests of a wavelet-based penetration control scheme demonstrated its potential applicability in preventing over travel of the drill bit during orthopedic surgery.

In order to enhance the reliability of the bone breakthrough detection, Lee and Shih proposed that feed force control should be implemented for regulating drilling torque at all times of drilling [4]. Not only thrust force information, but also drilling torque and feed rate was used together for judging the breakthrough. Using a 3-axis robotic bone drilling system, which consisted of a combined inner loop fuzzy controller for position control and outer loop PD controller for the feed unit force control, the state of penetration before the drill bit (twist drill bit) penetrated out of the bone could be identified with the threshold information of the thrust force, the trend of the drilling torque, and the feed rate of the drill.

Rather than relying on the thrust force and drilling torque information like in many other earlier proposed schemes, Osa et al. proposed an autonomous penetration detection scheme for cutting and drilling bones with hand-held tools [11,12]. Since an electric drill was utilized, it was possible to use the current flowing to the motor of the drill and the rotational speed of the tool to recognize the penetration with a support vector machine (SVM) algorithm. Test results of this scheme with spherical burr demonstrated that, not only thrust force and drilling torque, but also current and drill speed can be important indicators for recognizing states of bone penetration.

For most of the previously proposed drilling systems, real-time feedforce information is required for breakthrough detection. Thus, the installation of a force sensing instrument in the drilling system is essential [1,3,4,8–10,13–17]. In our research, the study of drilling mechanics leads to the proposition of an alternative scheme developed for bone drilling procedures that use a twist drill bit (the most widely used drilling tool in orthopedic surgery). This new scheme requires neither the installation of a force sensor nor the measurement of feed force. The novelty of the scheme is based on the integration of three key elements: current sensing, stepwise drilling, and hysteresis thresholding. A prototype of a drilling tool equipped with electronics for current sensing and signal conditioning has been shown to perform successful drilling while achieving effective breakthrough detection without force measurement.

#### 2. Breakthrough detection technique

#### 2.1. Current measurement for breakthrough detection

According to the physical operation of an electric drill, an increment of drilling torque load while drilling causes the motor driving the drill spindle to consume more current. However, when the breakthrough is occuring, the torque load declines, causing the current to reduce simultaneously. In principle, this phenomenon allows breakthrough to be detected based on the monitoring only of the motor current. A simple indicator for identifying the breakthrough involves a threshold value which can be determined slightly higher than the amount of current at no load. When the current flowing to the motor diminishes to such a value (usually during the occurrence of the breakthrough), the breakthrough is detected.

Breakthrough detection based on current measurement is considered an effective approach since, in typical set-ups, the current responds to torque load change very quickly. The measurement of current is also simple since it can be carried out without need of modifying the structure of the drill to install a sensor. Instead, it can be realized by connecting the drill with a current sensing circuit.

#### 2.2. Analysis of breakthrough detection scheme

To analyze the motor current behavior, a mathematical model of a direct current (DC) motor driving the drill chuck with direct transmission of power (without gearing) is considered. This model includes the following governing equations [18]:

$$\frac{d}{dt}i_a = -\frac{R_a}{L_a}i_a - \frac{k_v}{L_a}\omega + \frac{V_a}{L_a} \tag{1}$$

$$\frac{d}{dt}\omega = \frac{k_t}{I}i_a - \frac{b_m}{I}\omega - \frac{1}{I}T_L,\tag{2}$$

where  $i_a$  represents current flowing through the armature winding of the motor,  $R_a$ ,  $L_a$ , and  $V_a$  are resistance, inductance, and voltage of the armature winding,  $k_v$  is back electromotive force (emf) constant,  $\omega$  is rotational speed of the drill,  $k_t$  is torque constant of the motor, J is effective moment of inertia of the rotating parts,  $b_m$  is viscous friction coefficient of the motor, and  $T_L$  is torque load caused by drilling. Eqs. (1) and (2) may be expressed in the Laplace domain as

$$I_a(s) = \frac{1}{L_a s + R_a} (V_a(s) - k_v \Omega(s)) \tag{3}$$

$$\Omega(s) = \frac{1}{Js + b_{m}} (k_{t} I_{a}(s) - T_{L}(s)), \tag{4}$$

where  $I_a(s)$ ,  $V_a(s)$ ,  $\Omega(s)$ , and  $T_L(s)$  represent the Laplace transforms of  $i_a$ ,  $V_a$ ,  $\omega$ , and  $T_L$  respectively. By substituting (4) into (3) and rearranging, an expression for  $I_a(s)$  can be determined as

$$\begin{split} I_{a}(s) &= \frac{Js + b_{m}}{L_{a}Js^{2} + (L_{a}b_{m} + R_{a}J)s + (R_{a}b_{m} + k_{v}k_{t})}V_{a}(s) \\ &+ \frac{k_{v}}{L_{a}Js^{2} + (L_{a}b_{m} + R_{a}J)s + (R_{a}b_{m} + k_{v}k_{t})}T_{L}(s). \end{split} \tag{5}$$

Eq. (5) indicates that current change occurs in relation to the voltage of the armature winding  $V_a(s)$  and torque load  $T_L(s)$ . If voltage  $V_a$  is regulated to a constant value by the voltage-source power supply, changes of current will depend only on the torque load. When the drill experiences no load, the current is usually steady at a constant value (no-load current value). Afterward, when the drill bit progresses into the bone, the torque load acts at the tip of the drill causing the current to increase. Finally, when the drill is breaking through the bone, torque load will significantly diminish, causing the current to drop. Significant reduction of current therefore indicates the occurrence of the breakthrough.

#### 3. Realization of breakthrough detection

#### 3.1. Current sensing and signal conditioning circuit

In practice, the level of current flowing through the motor may be determined by the use of a sense resistor. Fig. 1 shows a sense resistor connected in series with the motor. The voltage across this sense resistor is the sensing signal which is processed by a signal conditioning circuit comprising an isolation amplifier, a differential amplifier, and an instrumentation amplifier. The isolation amplifier associated with input filter components is used to perform initial filtering for suppressing high-frequency noise while providing electrical isolation between the power line and other parts of the signal conditioning circuit. The output of the isolation amplifier is processed by a unity-gain differential amplifier with associated capacitors for further noise filtering. These filtering components are included for suppressing commutation ripple before the signal is offset and amplified to the required level by an instrumentation amplifier. Fig. 2 shows the schematic of the circuit. In the Laplace domain, the voltage across the sense resistor  $V_{\rm sr}(s)$  is an analog signal whose magnitude varies with the amount of current flowing through the motor according to

$$V_{sr}(s) = R_{sr}I_a(s). (6)$$

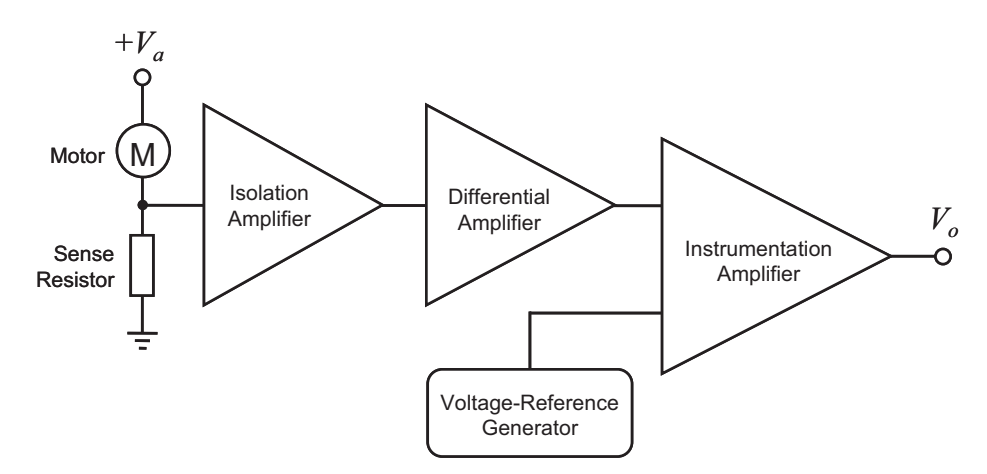


Fig. 1. Main components of current sensing and signal conditioning circuit.

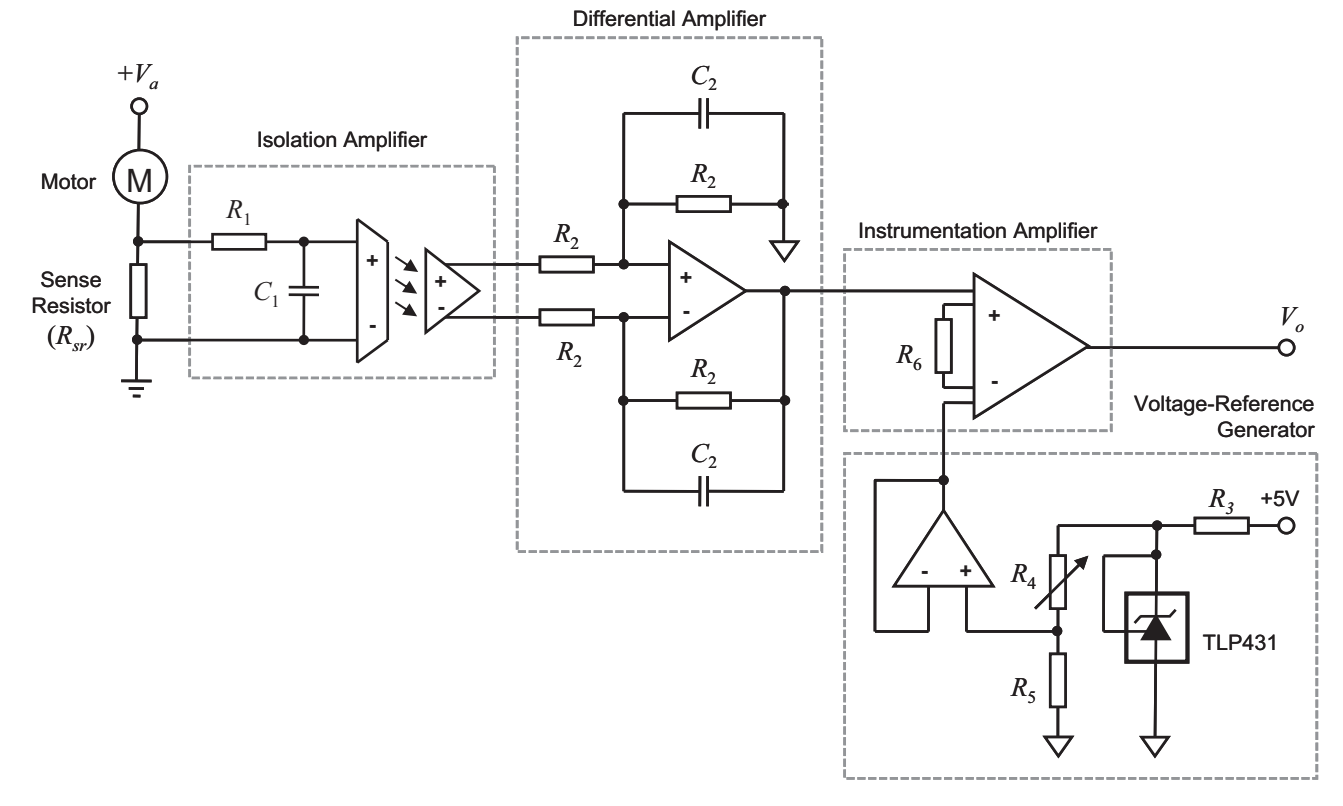


Fig. 2. Current sensing and signal conditioning circuit.

The analog signal  $V_{sr}(s)$  is filtered, amplified, and offset by the signal conditioning circuit to obtain the voltage output  $V_o$  which is given by

$$V_o(s) = k_2 [k_1 V_{sr}(s) - V_{ref}(s)]. \tag{7}$$

In this equation,  $k_1$  and  $k_2$  are gains of the isolation amplifier and the instrumentation amplifier respectively.  $V_{ref}(s)$  is the constant reference voltage obtained from a precision voltage reference generator. The voltage from this device is used to adjust the offset of  $V_{sr}(s)$  after high frequency noise is filtered out. Substituting  $V_{sr}(s)$  in (7) and using (5), we obtain

$$\begin{split} V_o(s) &= k_2 \big[ k_1 R_{sr} I_a(s) - V_{ref} \big] \\ &= k_2 k_1 R_{sr} I_a(s) - k_2 V_{ref} \\ &= \frac{k_2 k_1 R_{sr} J s + k_2 k_1 R_{sr} b_m}{L_a J s^2 + (L_a b_m + R_a J) s + (R_a b_m + k_v k_t)} V_a(s) \\ &+ \frac{k_v k_2 k_1 R_{sr}}{L_a J s^2 + (L_a b_m + R_a J) s + (R_a b_m + k_v k_t)} T_L(s) - k_2 V_{ref}. \end{split} \tag{8}$$

It should be noted that, transient effects from electronic components (including filters and amplifiers) are neglected here since their responses are much faster than that of the motor. In (8), if  $V_{ref}(s)$  is set such that the magnitudes of the first and the last terms become close to each other in steady state, the voltage output  $V_0(s)$  can be simply determined as

$$V_o(s) \approx \frac{k_v k_2 k_1 R_{sr}}{L_a J s^2 + (L_a b_m + R_a J) s + (R_a b_m + k_v k_t)} T_L(s). \tag{9}$$

For typical small-sized low-inertia DC motors, the transfer function obtained from (9) behaves as a low-pass filter having high bandwidth due to the existence of fast system poles. This property gives good characteristics for measuring transient features of the torque load profile. The variation in voltage output  $V_0$  for a typical drilling torque load, produced when the drill bit penetrates into an object in short quick steps until the breakthrough is reached, is shown in Fig. 3. It can be seen that the voltage output responds to the changing torque load very quickly to produce a clear peak each time the drill is

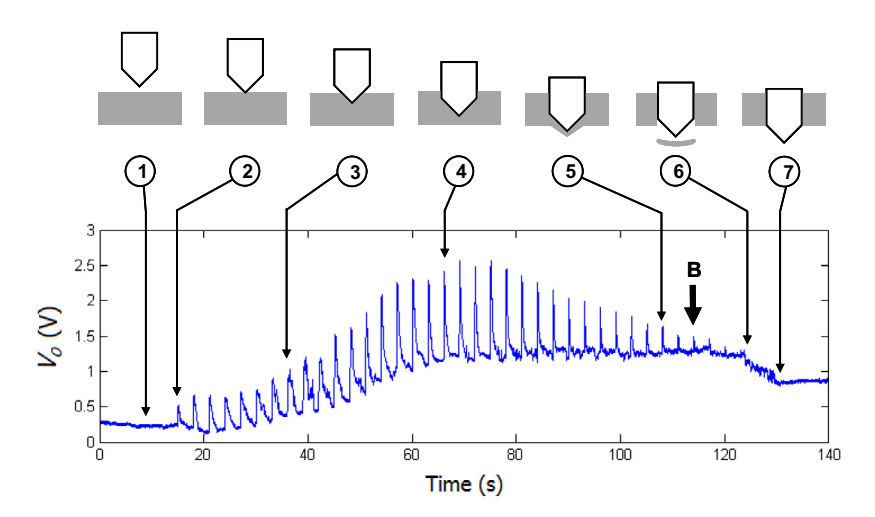


**Fig. 3.** Typical voltage output  $V_o$  recorded while drilling a flat plate with a twist drill bit: 1) no contact between the drill bit and the object, 2) the peak of the first drilling step arising when the tip of the drill bit first penetrates into the object, 3) half of the conical tip of the drill bit penetrating into the object, 4) conical tip of the drill bit completely penetrating into the object and 5) thin layer of material bent out at the bottom of the hole, 6) the tip of the drill bit breaking out of the object (complete breakthrough), and 7) conical tip of the drill bit completely penetrating out of the object.

advanced. This behavior can be exploited for accurate detection of the breakthrough.

#### 3.2. Breakthrough detection algorithm

To identify breakthrough, the magnitude of the voltage output  $V_o$  is sampled and the breakthrough detection algorithm applied. This algorithm is designed to detect the breakthrough when executing stepwise drilling. This drilling procedure involves a controlled motion of the drill

such that a sub-millimeter increase in drilling depth occurs for each step. Several successive drilling steps are carried out until the breakthrough occurs. Because the drill movement is stepwise, drilling torque load is approximately periodic (see the plot in Fig. 3). While executing each drilling step, there is a sharp peak in the torque load. Each peak also produces a peak in the voltage output signal. Several steps of drilling are executed until the tip of the drill is about to break out of the object being drilled. The magnitude of the peak then declines. By applying an algorithm based on the measurement of the peaks, the breakthrough

Start Record *n* initial values of  $V_o$  and calculate the average  $\rightarrow V$ Move the drill 1 step toward the bone while recording m highest Initial Drilling Phase sampled values of  $V_a$  and calculate the average  $\rightarrow$ False The drill is within safety range True False True Record *n* initial values of  $V_a$  and calculate the average  $\rightarrow V_a$ Main Drilling & Breakthrough Phases Move the drill 1 step toward the bone while recording m highest sampled values of  $V_a$  and calculate the average  $\rightarrow$ The drill is within False safety range True False  $\hat{V_o} - \overline{V_o} < V_{th2}$ True Stop

Fig. 4. Breakthrough detection algorithm.

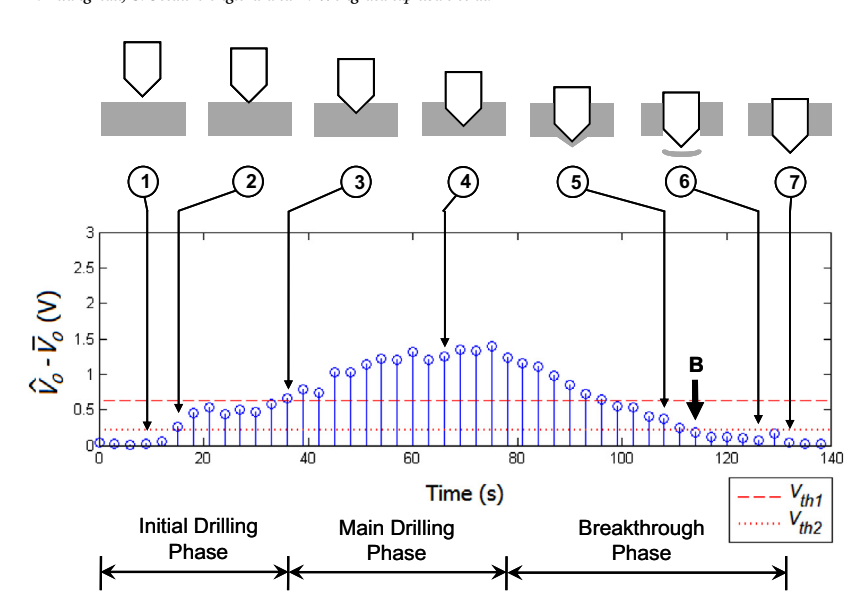


**Fig. 5.** Typical plot of the difference between  $\hat{V_o}$  and  $\overline{V_o}$  (denoted as  $\hat{V_o} - \overline{V_o}$ ) with indication of drilling states (see Fig. 3). The breakthrough is detected when  $\hat{V_o} - \overline{V_o}$  becomes lower than the secondary threshold  $V_{th2}$  (marked as "B").

can therefore be detected when the magnitude of the peak diminishes to zero.

In practice, contamination of noise in the sampled signal occurs. An averaging technique for noise reduction is therefore applied during the process of breakthrough identification. As shown in Fig. 4, n initial values of  $V_0$  are recorded prior to feeding the drill toward the object. The average of these initial values represents the minimal value of  $V_o$ , denoted as  $\overline{V_0}$ . After recording these values, the drill is fed toward the object with a small increase in drilling depth over a short period of time  $(t_{\text{feed}})$ . In the initial drilling phase, if the tip of the drill bit does not contact with the object, the torque load remains zero. Short stepwise feeds are repeated (as long as the drill does not move beyond a predefined allowable safety range) until the tip of the drill bit comes into contact with the object. The time period for each repetition of a stepwise feed  $(t_{
m repeat})$  is set sufficiently long to complete a small drilling step  $(t_{
m repeat}>>$  $t_{\rm feed}$ ) that is required to cut and remove material out of the drilled hole. When the lips (cutting edges at the tip) of the drill bit begin cutting into the object, the torque load rapidly increases causing  $V_0$  to increase to a peak value and then decline (see the plot in Fig. 3). For the advantage of noise immunity, an average is also calculated to estimate the peak of the signal based on the m highest sampled values of  $V_o$  recorded during advancement of the drill. This average is denoted as  $\widehat{V_o}$ . The value of  $\widehat{V_o}$ is compared to the averaged initial value,  $\overline{V_o}$ . If the difference between these two values is higher than the primary threshold value  $(\widehat{V_0} - \overline{V_0})$  $V_{th1}$ ), the drill is recognized to be in the main drilling phase (see Fig. 5). Based on experimental verifications, a practical value of the primary threshold  $V_{th1}$  can be determined as the voltage difference  $\widehat{V}_{o} - \overline{V}_{o}$  when half of the conical tip of the drill bit penetrates into the object. When the penetration is deeper than half of the conical tip of the drill bit, it is considered to be in the main drilling phase. Stepwise drilling motion then continues while the algorithm keeps monitoring the voltage difference  $\widehat{V_o} - \overline{V_o}$ . The voltage difference  $\widehat{V_o} - \overline{V_o}$  usually remains higher than  $V_{th1}$  until the breakthrough starts to occur. In the breakthrough phase, the voltage difference  $\widehat{V}_o - \overline{V}_o$  reduces successively. If the difference between  $\widehat{V}_o$  and  $\overline{V}_o$  drops to zero, the complete breakthrough is reached. However, another threshold—the secondary threshold  $(V_{th2})$ —is set to recognize the early state of the breakthrough. If the voltage difference  $\widehat{V}_{o} - \overline{V}_{o}$  becomes less than this secondary threshold value  $(\widehat{V}_{o} - \overline{V}_{o} < V_{th2})$ , the breakthrough state is detected, as shown in Fig. 5.

To negate the measurement uncertainty that might lead to fault breakthrough detection in practice,  $V_{th2}$  should be set slightly higher than the upper deviation of the voltage differences  $\widehat{V_o} - \overline{V_o}$  when the drill has no drilling load. Higher value of  $V_{th2}$  may be set for early detection of the breakthrough, allowing a safety margin to prevent over drilling in

critical surgical procedures. It should be noted that, according to the hysteresis thresholding principle,  $V_{th2}$  and  $V_{th1}$  form the lower and upper thresholds for breakthrough state recognition with uncertainty immunity. Since the voltage differences  $\widehat{V_o} - \overline{V_o}$  can fluctuate due to electrical noise, mechanical vibration, and inhomogeneity of bone, having large difference band between  $V_{th1}$  and  $V_{th2}$  by keeping  $V_{th2}$  low is essential for maintaining high reliability of breakthrough detection. In practice, the achievable difference band is dependent on the properties of the drilled material.

#### 4. Experimental verifications

#### 4.1. Drill prototype

The breakthrough detection scheme was tested using a drill prototype which is composed of an electric drill with a twist drill bit, associated electronics, and a drill stand. Fig. 6 depicts this prototype with

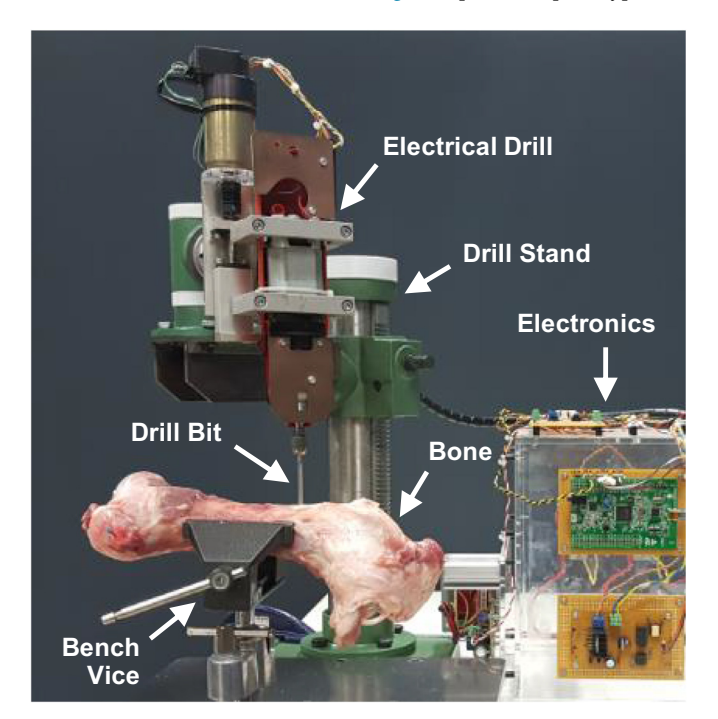


Fig. 6. Drill prototype and a piece of bone specimen.

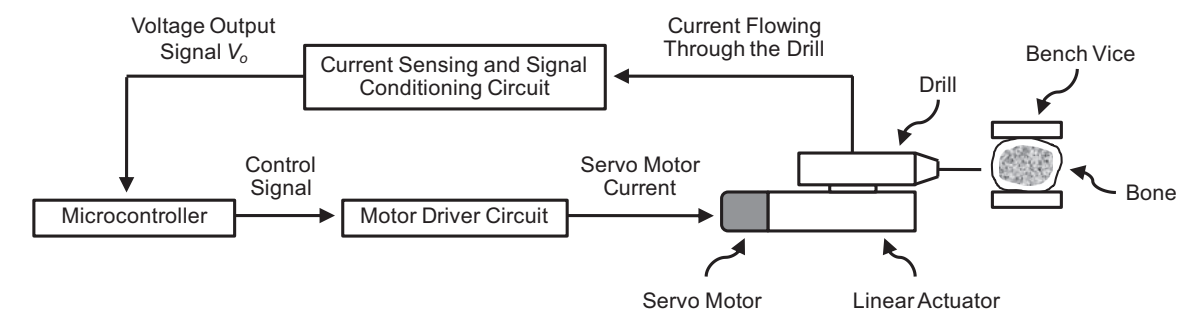


Fig. 7. Architecture of the control system.



Fig. 8. Comparison of drilled holes on acrylic plates. Left: the holes drilled with breakthrough detection algorithm (residual thin layer of acrylic at the bottom of the holes still remains as seen in white). Middle: bottom of the holes drilled with breakthrough detection algorithm (residual thin layer of acrylic at the bottom of the holes clearly seen in white). Right: the holes drilled without breakthrough detection algorithm (no residual layer of acrylic remains since the acrylic plate was drilled through).

a piece of bone specimen clamped in place by a bench vice. The architecture of the control system associated with this prototype is shown in Fig. 7. The main component of the drill is a permanent magnet DC motor which is coupled directly with the drill chuck without speed control. It is installed on a 1-mm-pitch ball-screw linear actuator driven by a DC servo motor (Faulhaber Schonaich 3557K024CS). To perform precise control of the drill feed motion, a proportional-integral-derivative (PID) control algorithm is implemented in a 32-bit microcontroller (STM32F407VG) combined with an H-bridge motor driver circuit. This motion control algorithm was tuned to provide an overdamped response with rise time of 24 ms. Operating at a sampling frequency of 1 kHz, the microcontroller uses its internal 12-bit analog-to-digital converter for sampling the analog signal from the breakthrough detection circuit such that, as soon as the occurrence of the breakthrough is detected, it can control the drill bit to move out of the drilled hole.

#### 4.2. Experiments

Two drilling experiments were conducted with the drill prototype to verify the breakthrough detection and control algorithms. The first experiment was conducted with acrylic plates. The other experiment was conducted with porcine bones. To carry out these experiments, a 3.2-mm twist drill bit was used. The drill was controlled to move step-by-step with a step size of 0.1 mm and time period of 3 s while the drill chuck rotated at a speed of 7950 rpm (no-load speed). Note that step size is one of the key parameters for successful breakthrough detection since it affects both detectability and precision of the breakthrough detection scheme. Small step size is mostly desirable since it increases the positional precision. However, if the step size is too small, the detectability of breakthrough detection and immunity to uncertainty will be poor due to reduced current peaks. On the contrary, if step size is big, the detectability is high but the precision is low due to reduced motion control resolution. Depending on the application, different step sizes may be set based on target criterion for the tradeoff between detectability and precision. Equipment associated with these two experiments is as shown in Fig. 6. Details and results of each experiment are described as follows:

1) Drilling acrylic plates. Three pieces of 3-mm-thickness transparent acrylic plates were used as specimens. The first two pieces were used for breakthrough detection tests. Each specimen was clamped on a bench vice while drilling was controlled according to the breakthrough detection algorithm shown in Fig. 4. The third piece of specimen was used for drilling holes through without breakthrough detection. In breakthrough detection tests, the values of  $\widehat{V_o}$  and  $\overline{V_o}$  were individually calculated from 5 sampled values (n = m = 5). The primary threshold  $V_{th1}$  was set to 0.6  $V_{\underline{th1}} = 0.6$ ) which is approximately equal to the voltage difference  $\widehat{V}_{o} - \overline{V}_{o}$  observed when half of the conical tip of the drill bit penetrated into the acrylic plates. The secondary threshold  $V_{th2}$  was set to 0.2 V  $(V_{th2} = 0.2)$  enabling early detection of the breakthrough to be carried out. Note that the value of this secondary threshold is higher than the upper deviation of the voltage differences  $\widehat{V}_{o} - \overline{V}_{o}$  when the drill has no drilling load as described in Section 3.2. When the breakthrough occurred, the drill bit was removed from the drilled hole immediately. Only a small residual layer of acrylic remained at the bottom of the hole. The drilling operation was repeated for ten drilled holes (five holes on each acrylic plate). The holes drilled with and without the breakthrough scheme are shown in Fig. 8. Table 1 shows the thicknesses of the residual layer of acrylic obtained from each time of drilling. The average is approximately 0.19 mm. This result shows that slightly early detection before the occurrence of complete breakthrough is precisely carried out with the thresholds specified based on the described criterion.

**Table 1**Thicknesses of the residual layers of acrylic remaining at the bottom of the drilled holes.

Hole No.	Thickness (mm)	Hole No.	Thickness (mm)
1	0.17	6	0.21
2	0.17	7	0.22
3	0.18	8	0.22
4	0.19	9	0.22
5	0.19	10	0.17
	Average		0.19
	Standard Deviation		0.02

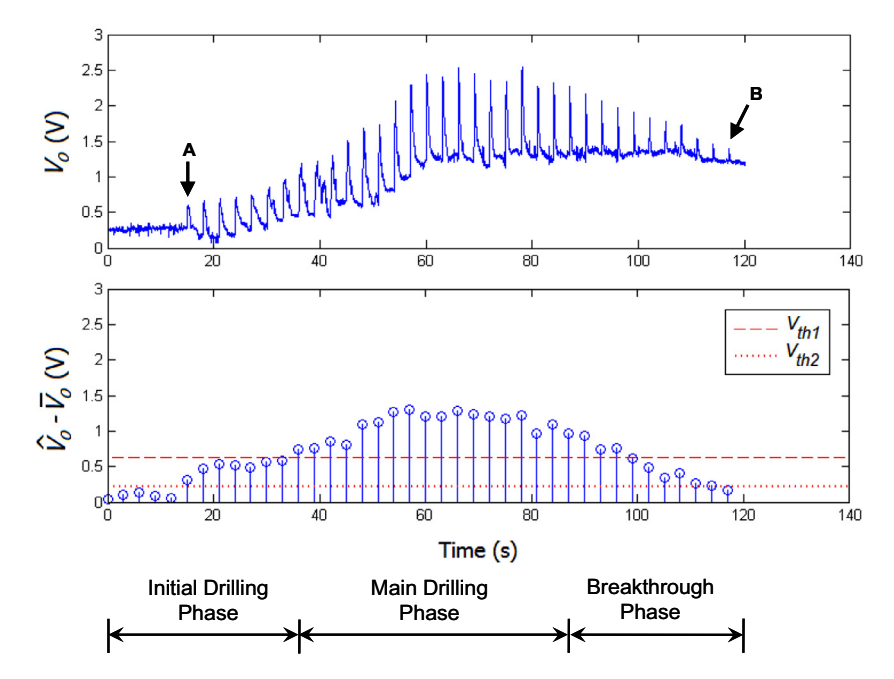


**Fig. 9.** Typical voltage output  $V_o$  recorded during drilling a hole on an acrylic plate (top) and the associated plot of  $\hat{V_o} - \overline{V_o}$  (bottom). A: the peak of the first drilling step and B: the peak of the last drilling step when the breakthrough is detected.

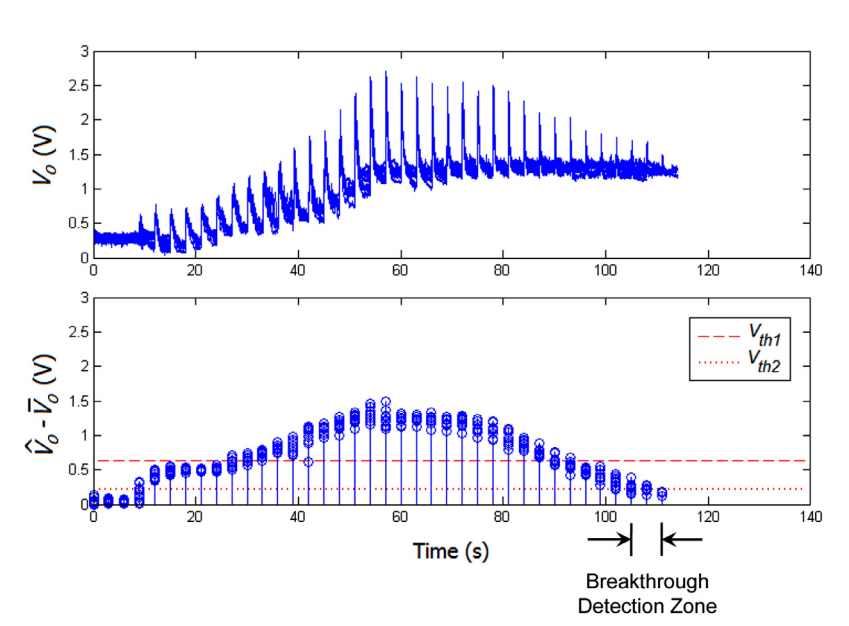
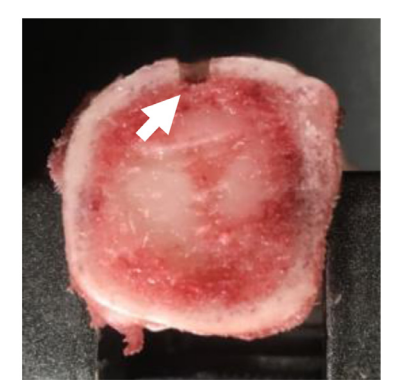


Fig. 10. Overlaying plots of all ten drilling operations and breakthrough detection zone in which the voltage differences  $\hat{V_o} - \overline{V_o}$  become lower than  $V_{th2}$ .

In Fig. 9, a typical voltage output  $V_o$  and voltage difference  $\widehat{V_o} - \overline{V_o}$ recorded throughout the operation of drilling is shown. As can be seen, after several steps of drilling, the peak voltage value of each drilling step declined. Drilling was terminated when the voltage difference  $\widehat{V}_{o} - \overline{V}_{o}$ dropped below the secondary threshold  $V_{th2}$ . Thirty-five drilling steps, equivalent to the travel distance of 3.5 mm, was executed before the breakthrough was detected. This exceeds the thickness of the acrylic plate (3.0 mm) because the residual layer of acrylic was bent out at the bottom of the hole before complete breakthrough occurred (see Figs. 3 and 5). Fig. 10 illustrates overlaying plots of all ten drilling operations showing the consistency of the voltage signals and breakthrough detection zone in which the voltage differences  $\widehat{V}_o - \overline{V}_o$  become lower than  $V_{th2}$ . It is clear that, after 33–35 drilling steps, the breakthrough was detected in this zone. The deviation of breakthrough detection is therefore less than 3 drilling steps or, in other word, within 0.3 mm (step size = 0.1 mm).

2) Drilling porcine bones. Four pieces of femur bones were used as specimens in the second experiment. Every specimen has two distinct





**Fig. 11.** Drilled hole on the femur bone (left) and the cross-section of the hole on the bone (right).

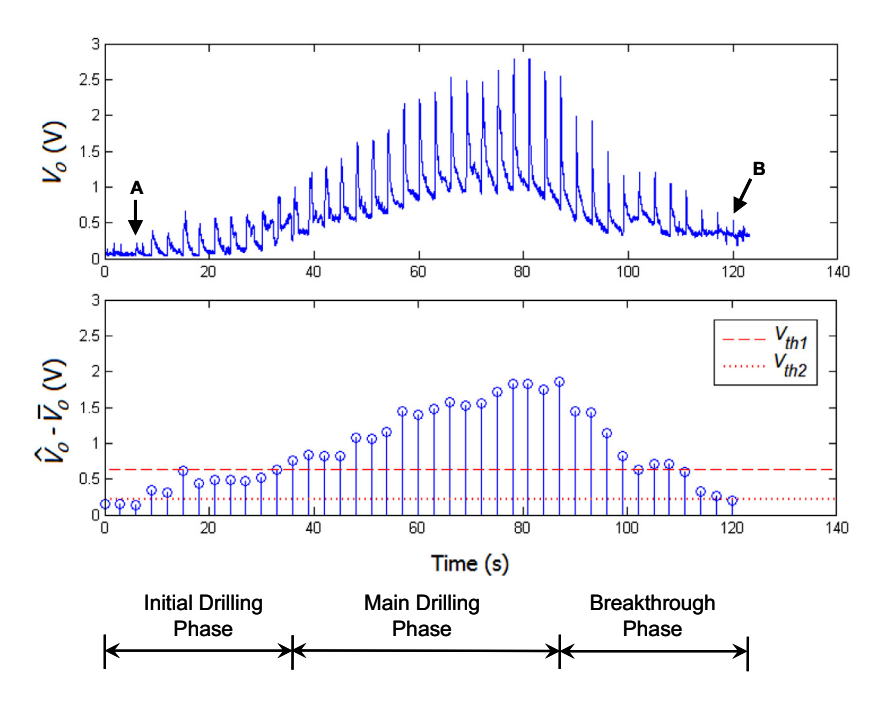


**Fig. 12.** Typical voltage output  $V_o$  recorded during drilling a hole on a femur bone (top) and the associated plot of  $\hat{V_o} - \overline{V_o}$  (bottom). A: the peak of the first drilling step and B: the peak of the last drilling step when the breakthrough is detected.

bone layers: cortical bone layer (the outer hard layer) and cancellous bone layer (the inner soft porous layer). While performing drilling, each bone was clamped in place. The same settings for all parameters including the spindle speed were applied in this case as in the previous experiment. In this experiment, the objective was to detect the breakthrough when the drill bit started to penetrate out of the cortical bone to the inner porous layer of the cancellous bone. After several steps of drilling, the breakthrough was successfully detected. Fig. 11 shows a typical drilled hole and the bone cross-section. As can be seen from the figure, drilling stopped at the boundary of the cortical and cancellous bone layers. Very little damage to the cancellous bone was caused. The records of voltage output  $V_0$  and the voltage difference  $\widehat{V_0} - \overline{V_0}$  associated with this experiment are shown in Fig. 12. Compared to the case of drilling acrylic plates, the response of the measurement signal in this case has a more irregular pattern. This was mainly due to the inhomogeneous structure of the bone material. In Fig. 13, the cross-sections of



Fig. 13. Cross-sections of drilling holes on four different pieces of femur bones.

drilled holes on four different pieces of bones are shown. It is clear that only little damage was caused to the cancellous bones because the conical tip of the drill bit travelled only slightly beyond the boundary of the cortical and cancellous bones, and was stopped before complete cuts of the cortical bones by the cutting edges at the tip of the drill bit were made.

#### 5. Conclusion

In this research, the combination of three key techniques is proposed for breakthrough detection in bone drilling procedures: 1) measurement of current flowing though the motor of the electric drill using a sense resistor, 2) stepwise drilling action controlled by a microcontroller, and 3) hysteresis thresholding for breakthrough detection with uncertainty immunity. The measurement of current can be performed effectively by applying a sense resistor with specially designed signal conditioning circuit, which is composed of an isolation amplifier, a unity-gain differential amplifier with input filter components, and an instrumentation amplifier. With the stepwise drilling action, there is a peak in the measurement signal at each step of drilling. By monitoring the peak, the breakthrough can be identified since, when the breakthrough begins to occur, the peaks at successive drilling steps decline. If the peak declines below threshold values according to the hysteresis thresholding principle, the drilling process is terminated and the drill bit removed from the drilled hole. This drilling procedure allows safe drilling to be executed. For real surgery, severe damage of soft tissue underneath the hard layer of bone can be prevented.

A number of drilling experiments with acrylic plates and porcine bones showed that threshold values are important parameters for successful breakthrough detection. When they are properly specified, the breakthrough can be effectively detected in real-time with the proposed scheme. However, the main limitation of this scheme is that tuning of detection parameters for specific bone types and drilling conditions associated with different drill bit sizes and shapes is required. Initially, this would be done based on empirical data from calibration testing on sample bone specimens. Over time, compiling a large set of test results will allow more general tuning rules to be established. Moreover, further investigations on the effects of spindle speed, stiffness of the drill stand, and stiffness of the drilled object itself are required since they also influence threshold setting. Although twist drill bits are commonly used, other types of cutting tools for drilling such as spherical burrs,

round-nose end mills, and square end mills should also be tested for evaluation and further development of the breakthrough detection scheme.

#### **Declaration of Competing interest**

The authors have no affiliation with any organization with a direct or indirect financial interest in the subject matter discussed in the manuscript.

#### Acknowledgements

This work was supported by Chiang Mai University, Thailand's Office of the Higher Education Commission (OHEC), and the Thailand Research Fund (TRF) [grant number MRG5980212].

#### References

- [1] Brett PN, Baker DA, Reyes L, Blanshard J. An automatic technique for micro-drilling a stapedotomy in the flexible stapes footplate. Proc Inst Mech Eng 1995;209(4):255–62 Part H: Journal of Engineering in Medicine.
- [2] Baker D, Brett PN, Griffiths MV, Reyes L. A mechatronic drilling tool for ear surgery: a case study of some design characteristics. Mechatronics 1996;6(4):461–77 1.
- [3] Allotta B, Giacalone G, Rinaldi L. A hand-held drilling tool for orthopedic surgery. IEEE/ASME Trans Mechatron 1997;2(4):218–29.
- [4] Lee WY, Shih CL. Control and breakthrough detection of a three-axis robotic bone drilling system. Mechatronics 2006;16(2):73–84.
- [5] Brett PN, Taylor RP, Proops D, Coulson C, Reid A, Griffiths MV. A surgical robot for cochleostomy. In: Proceedings of the 29th annual international conference of the IEEE EMBS; 2007. p. 1229–32.
- [6] Kotev V, Boiadjiev G, Kawasaki H, Mouri T, Delchev K, Boiadjiev T. Design of a hand-held robotized module for bone drilling and cutting in orthopedic surgery. Design of a hand-held robotized module for bone drilling and cutting in orthopedic surgery. In: Proceedings of the IEEE/SICE international symposium on system integration (SII); 2012. p. 504–9.
- [7] Díaz I, Gil JJ, Louredo M. Bone drilling methodology and tool based on position measurements. Comput Methods Progr Biomed 2013;112(2):284–92.
- [8] Ong FR, Bouazza-Marouf K. The detection of drill bit break-through for the enhancement of safety in mechatronic assisted orthopaedic drilling. Mechatronics 1999;9(6):565–88.
- [9] Allotta B, Belmonte F, Bosio L, Dario P. Study on a mechatronic tool for drilling in the osteosynthesis of long bones: tool/bone interaction, modeling and experiments. Mechatronics 1996;6(4):447–59.
- [10] Colla V, Allotta B. Wavelet-based control of penetration in a mechatronic drill for orthopaedic surgery. In: Proceedings of the IEEE international conference on robotics and automation (ICRA); 1998. p. 711–16.
- [11] Osa T, Abawi CF, Sugita N, Chikuda H, Sugita S, Ito H, Moro T, Takatori Y, Tanaka S, Mitsuishi M. Autonomous penetration detection for bone cutting tool using demonstration-based learning. In: Proceedings of the IEEE international conference on robotics and automation (ICRA); 2014. p. 290–6.
- [12] Osa T, Abawi CF, Sugita N, Chikuda H, Sugita S, Tanaka T, Oshima H, Moro T, Tanaka S, Mitsuishi M. Hand-held bone cutting tool with autonomous penetration detection for spinal surgery. IEEE/ASME Trans Mechatron 2015;20(6):3018–27.
- [13] Hu Y, Jin H, Zhang L, Zhang P, Zhang J. State recognition of pedicle drilling with force sensing in a robotic spinal surgical system. IEEE/ASME Trans Mechatron 2014;19(1):357–65.
- [14] Jiang Z, Sun Y, Zhao S, Hu Y, Zhang J. A model of vertebral motion and key point recognition of drilling with force in robot-assisted spinal surgery. In: Proceedings of the IEEE/RSJ international conference on intelligent robots and systems (IROS); 2017. p. 6455–62.

- [15] Qi L, Meng MQ. Real-time break-through detection of bone drilling based on wavelet transform for robot assisted orthopedic surgery. In: Proceedings of the IEEE international conference on robotics and biomimetics (ROBIO); 2014. p. 601–6.
- [16] Sun Y, Jin H, Hu Y, Zhang P, Zhang J. State recognition of bone drilling with audio signal in robotic orthopedics surgery system. In: Proceedings of the IEEE/RSJ international conference on intelligent robots and systems (IROS); 2014. p. 3503–8.
- [17] Jin H, Hu Y, Deng Z, Zhang P, Song Z, Zhang J. Model-based state recognition of bone drilling with robotic orthopedic surgery system. In: Proceedings of the IEEE international conference on robotics and automation (ICRA); 2014. p. 3538–43.
- [18] Kuo BC, Golnaraghi F. Automatic control systems. 8th ed. New York: John Wiley & Sons; 2003.



Pinyo Puangmali received the B.Eng. degree in mechanical engineering from Chiang Mai University, Chiang Mai, Thailand, in 1999. He received the M.Sc. degree in mechatronics from the University of Siegen, Germany, in 2004 and the Ph.D. degree in mechanical engineering from King's College London, University of London, U.K., in 2011. Since 2011, he has been with the Department of Mechanical Engineering, Chiang Mai University, where he is currently an Assistant Professor. His research interests include mathematical modeling of dynamic systems, mechatronics, and robotics.



Somphop Jetdumronglerd received the B.Eng. degree in mechanical engineering from Chiang Mai University, Chiang Mai, Thailand, in 2012. He is currently working toward the M.Eng. degree in the area of mechatronics at Chiang Mai University. His research interests include mechatronic and robotic systems.



Theeraphong Wongratanaphisan received the B.Eng. degree in mechanical engineering from Chiang Mai University, Chiang Mai, Thailand, in 1993. He received the M.S. and Ph.D. degrees in mechanical engineering from Lehigh University, U.S.A. in 1996 and 2001, respectively. Since 1994, he has been with the Department of Mechanical Engineering, Chiang Mai University, where he is currently an Associate Professor. His research interests include system design, control, and robotics.



Matthew O. T. Cole received the M.A. degree in natural sciences from the University of Cambridge, Cambridge, U.K., in 1995. He received the M.Sc. and Ph.D. degrees in mechanical engineering from the University of Bath, Bath, U.K., in 1995 and 1999 respectively. Since 2003, he has been a Faculty Member at Chiang Mai University, Chiang Mai, Thailand, where he is a Professor in the Department of Mechanical Engineering. His research interests include the application of signal processing and control technology in machine systems.